Nano Research

ISSN 1998-0124 CN 11-5974/O4
https://doi.org/10.1007/s12274-021-3561-2

Research Article

Sulfur-doped graphene anchoring of ultrafine Au_{25} nanoclusters for electrocatalysis

Mufan Li[1,3,§], Bei Zhang[1,§], Tao Cheng[5], Sunmoon Yu[2,3], Sheena Louisia[1,3], Chubai Chen[1], Shouping Chen[2], Stefano Cestellos-Blanco[2], Miquel Salmeron[3], William A. Goddard III[5], and Peidong Yang[1,2,3,4] (✉)

Nano Res., **Just Accepted Manuscript** • https://doi.org/10.1007/s12274-021-3561-2
http://www.thenanoresearch.com on May. 3, 2021

Just Accepted

Address correspondence to First A. Firstauthor, email1; Third C. Thirdauthor, email2

TABLE OF CONTENTS (TOC)

Sulfur-doped Graphene Anchoring of Ultrafine Au_{25} Nanoclusters for Electrocatalysis

Mufan Li [1,3,#], Bei Zhang[1,#], Tao Cheng[5], Sunmoon Yu[2,3], Sheena Louisia[1,3], Chubai Chen[1], Shouping Chen[2], Stefano Cestellos-Blanco[2], Miquel Salmeron[3], William A. Goddard III[5], Peidong Yang[1,2,3,4*]

[1] Department of Chemistry, University of Berkeley, California 94720, United States

[2] Department of Materials Science and Engineering, University of Berkeley, California 94720, United States

[3] Chemical Science Division, Lawrence Berkeley National Laboratory, Berkeley, California 94720, United States

[4] Kavli Energy NanoScience Institute, Berkeley, California 94720, United States

[5] Materials and Process Simulation Center, California Institute of Technology, Pasadena, California 91125, United States

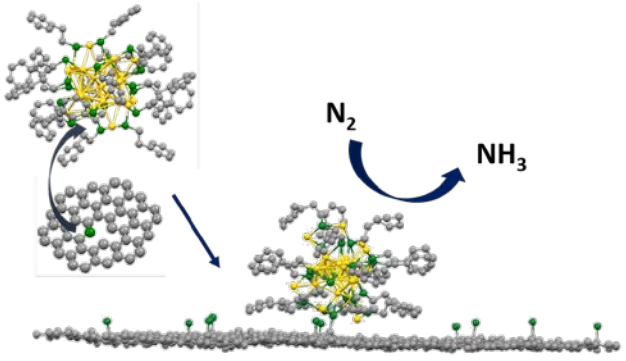

The anchoring effect origin from sulfur-doped graphene enables a significantly enhanced stability of ultrafine Au nanoclusters during electrocatalytic nitrogen reduction.

Nano Res (automatically inserted by the publisher)
DOI (automatically inserted by the publisher)
Research Article Please choose one

Sulfur-doped Graphene Anchoring of Ultrafine Au_{25} Nanoclusters for Electrocatalysis

Mufan Li [1,3,#], Bei Zhang[1,#], Tao Cheng[5], Sunmoon Yu[2,3], Sheena Louisia[1,3], Chubai Chen[1], Shouping Chen[2], Stefano Cestellos-Blanco[2], Miquel Salmeron[3], William A. Goddard III[5], Peidong Yang[1,2,3,4*](✉)

[1] Department of Chemistry, University of Berkeley, California 94720, United States

[2] Department of Materials Science and Engineering, University of Berkeley, California 94720, United States

[3] Chemical Science Division, Lawrence Berkeley National Laboratory, Berkeley, California 94720, United States

[4] Kavli Energy NanoScience Institute, Berkeley, California 94720, United States

[5] Materials and Process Simulation Center, California Institute of Technology, Pasadena, California 91125, United States

Received: day month year / Revised: day month year / Accepted: day month year (automatically inserted by the publisher)

ABSTRACT

The biggest challenge of exploring the catalytic properties of under-coordinated nanoclusters is the issue of stability. We demonstrate herein that chemical dopants on sulfur-doped graphene (S-G) can be utilized to stabilize ultrafine (sub-2 nm) $Au_{25}(PET)_{18}$ clusters to enable stable nitrogen reduction reaction (NRR) without significant structural degradation. The Au_{25}@S-G exhibits an ammonia yield rate of 27.5 μg NH_3 $mg_{Au}^{-1}h^{-1}$ at -0.5 V with faradic efficiency of 2.3%. More importantly, the anchored clusters preserve ~80% NRR activity after four days of continuous operation, a significant improvement over the 15% remaining ammonia production rate for clusters loaded on undoped graphene tested under the same conditions. Isotope labeling experiments confirmed the ammonia was a direct reaction product of N_2 feeding gas instead of other chemical contaminations. *Ex-situ* X-ray photoelectron spectroscopy and X-ray absorption near-edge spectroscopy of post-reaction catalysts reveal that the sulfur dopant plays a critical role in stabilizing the chemical state and coordination environment of Au atoms in clusters. Further ReaxFF molecular dynamics (RMD) simulation confirmed the strong interaction between Au NCs and S-G. This substrate-anchoring process could serve as an effective strategy to study ultrafine nanoclusters' electrocatalytic behavior while minimizing the destruction of the under-coordinated surface motif under harsh electrochemical reaction conditions.

KEYWORDS

Gold nanoclusters, sulfur-doped graphene, nitrogen reduction reaction, electrocatalysis, anchoring effect.

1 Introduction

The discrete electronic structure of small Nanoclusters (from 3~40 atoms) can lead to unique properties chemical and spectroscopic properties [1] [2] [3] [4]. Moreover, because of the under-coordinated surface they can display unique chemisorption behaviors compared with conventional large nanoparticle systems (>2 nm diameter) [5]. Thus the ultrafine (from sub-nanometer to ~2 nm) nanoclusters (NCs) have attracted growing interest for applications to such catalytic reactions, as selective hydrogenation [6], carbon dioxide reduction [7] [8, 9], and carbon monoxide oxidation [10]. However, the significant surface under-coordinating nature of NCs tends to induce the sintering and aggregation of the clusters with formation of larger particles during reaction, considerably altering the experimental size-reactivity relationship. Hence, a crucial challenge to exploit the intrinsic catalytic properties of NCs [11] is to achieve cluster stability.

Extensive studies have demonstrated that porous materials such as metal-organic framework (MOF) [12] [13] [14]and zeolite materials [15] can effectively interact and confine metallic clusters having just a few atoms. However, the low conductivity of these carrier materials prevents their use as electrochemical substrates. Moreover, for electrocatalytic systems Ostwald ripening can cause severe agglomeration and destruction of the NCs. Thus, an ideal substrate that can stabilize under-coordinated nanoclusters in a harsh electrocatalysis environment should feature two critical characteristics:

1) good electrical conductivity that allows the electron transfer process;

2) strong anchoring capability to maintain the overall structure of ultrafine NCs.

It is well-established that Au forms relatively strong bond with sulfur atoms [16] [17]. Herein, we use sulfur-doped graphene (S-G) to demonstrate a dopant-anchoring strategy that can effectively stabilize the ultrafine $Au_{25}(PET)_{18}$ cluster (abbreviated as Au_{25} for simplicity) for long term electrocatalysis. The Au_{25}@S-G exhibits remarkable stability for the nitrogen reduction reaction (NRR) with a superior ammonia production rate. *Ex-situ* structural characterizations confirmed that the morphology and chemical state of the ultrafine Au_{25} NCs are well maintained.

2 Experimental

2.1 Synthesis and isolation of $Au_{25}(PET)_{18}$

Neutral $Au_{25}(PET)_{18}$ nanocluster has been prepared by a modified method from a previously reported protocol [18]. $HAuCl_4 \cdot 3H_2O$ (19.7 mg, 0.05mmol) and TOAB (32.8 mg, 0.06 mmol) were dissolved in a round bottom flask with 5 mL of tetrahydrofuran. The solution was vigorously stirred for 15 min to form a dark red solution. Phenylethanethiol (34.5 mg, 0.25 mmol) was then added to the solution. A transparent solution was obtained after 30 min. $NaBH_4$ (18.9 mg, 0.5 mmol) was dissolved in 1mL ice-cold water and added immediately to the reaction mixture. The reaction was stopped after 24 h. The crude sample was precipitated by a large excessive of ice-cold water and washed with methanol 3 times to remove unreacted precursors and free TOAB. The crude sample was passed through a silica column and subsequent size-exclusion column to yield pure neutral $Au_{25}(PET)_{18}$ nanocluster. The purity of the sample is confirmed by UV-vis, ESI-MS analysis, and ^1H NMR. The UV-vis spectrum of $Au_{25}(PET)_{18}$ nanocluster shows the characteristic absorption at 402 nm, 459 nm, 639 nm, and 693 nm. ^1H NMR spectra of both TOAB and $Au_{25}(PET)_{18}$ were recorded. The NMR peaks of $Au_{25}(PET)_{18}$ are consistent with the reported spectrum, which differs from in $[Au_{25}(PET)_{18}]^- \cdot TOAB^+$.[1] The peaks of TOAB at 3.56(t), 2.41(s), 1.73(s), and 1.14 (d) were not detected in $Au_{25}(PET)_{18}$, confirming the complete removal of TOAB in $Au_{25}(PET)_{18}$.

2.2 Physical characterizations

Transmission electron microscopy (TEM) was carried out using Hitachi H-7650. Inductively coupled plasma optical emission spectroscopy (ICP-OES) was tested using PerkinElmer Optima 7000 DV. XPS (Thermo Scientific K-alpha) measurement was conducted using an Al Ka source.

Address correspondence to p_yang@berkeley.edu

2.3 Catalyst loading and electrode preparation

Purified $Au_{25}(PET)_{18}$ were dispersed in toluene solution and mixed with sulfur-doped graphene via vigorous stir (500 rpm) for 1 hour. The Au_{25}@S-G were blow-dried by N_2. For electrode preparation, Au_{25}@S-G was dispersed in a mixture of ethanol and Nafion 117 solution (volume ratio of 100:1) with a concentration of 1 $mg_{catalyst}$ mL^{-1} to form catalyst ink. The catalysts ink was drop cast on carbon paper (0.5 cm × 2 cm) on both sides. The mass of loaded Au was measured by inductively coupled plasma - optical emission spectrometry (ICP-OES).

2.4 Electrochemical measurements Electrochemical experiments

The nitrogen reduction reaction (NRR) experiments were carried out using a three-electrode Nafion membrane-separated H-cell on a BioLogic potentiostat system. A graphite rod and Ag/AgCl (3 M KCl) were used as counters electrode and a reference electrode, respectively. Note that both the Nafion membrane and graphite rod was pretreated in 5% H_2O_2 aqueous solution and ultrapure water at 80℃ for 2 hours. 0.05 M H_2SO_4 was used as the electrolyte. Prior to NRR testing, the catalyst was activated by 20 potential cycles between -0.2 V to 0.2 V in Ar-saturated electrolyte for activation. To remove the trace NH_3 impurity, ultrapure N_2 gas (99.99%) was bubbled through H_2SO_4 (1 M) aqueous solution before fed into the electrolyte. The electrolyte is saturated with N_2 for 30 minutes ahead of NRR experiments. During the NRR experiment, a constant N_2 flow (20 sccm) was fed into the electrolyte at the cathode side. All potentials were calibrated into values versus reversible hydrogen electrode (RHE) via HER/HOR CV scan using two platinum wires as WE and CE.

2.5 Determination of ammonia concentration

Indophenol blue method was used to determine the ammonia concentration in the electrolyte. The concentration of ammonia in the electrolyte was determined using the indophenol blue method with commercialized ammonia TNT830 vial test kit (Purchased from HACH). 5 mL electrolyte was added to the ammonia reagent vial. After inverting the cap, the vail was settled for 15 minutes before UV-Vis spectra was collected. The NH_3 production was indicated by the formation of indophenol blue, which was determined by the absorbance at 680 nm, with its concentration calibrated by a standard plot using a series of standard ammonium sulfate solutions. NMR measurements were done on a Bruker Avance 500 system with water suppression.

2.6 Isotope experiment

$^{15}N_2$ isotopic experiment was performed using the same setup with the only change to be the feeding gas was switch to $^{15}N_2$ gas. The cell was pre-purged with Ar for 30 min. The operation current at constant potential under $^{15}N_2$ was performed using the same potentiostat as above. The quantification of ammonia was accomplished by NMR of the post-reaction cathodic electrolyte.

3 Results and discussion

3.1 Synthesis and characterization of Au_{25}NCs and Au_{25}@ S-G

We first synthesize $Au_{25}(PET)_{18}$ nanoclusters via a conventional solution-phase method[18]. The synthesis protocol for NCs is illustrated in Figure 1a, with the experimental procedures detailed in SI Methods. The reaction time, temperature, and concentration of Au precursors were optimized to achieve good morphology and uniformity. The as-synthesized Au clusters were purified by passing through a silica column and subsequent size-exclusion column to yield pure neutral $Au_{25}(PET)_{18}$ nanocluster. Ultraviolet-visible spectroscopy (UV-vis) and electrospray ionization mass spectrometry (ESI-MS) analysis were used to confirm the sample's purity. As shown in Figure 1b, UV-vis spectrum of $Au_{25}(PET)_{18}$ nanocluster shows typical characteristic absorption peaks at 402 nm, 459 nm, 639 nm, and 693 nm (highlighted with the red dashes in Figure 1b), which agree with previous reported neutral $Au_{25}(PET)_{18}$ results [18]. ESI-MS

results (Figure 1c) confirm that the purified nanoclusters are $Au_{25}(PET)_{18}$ with atomic monodispersity, and the isotopic distribution patterns are consistent with simulated pattern of $Au_{25}(PET)_{18}$ (Fig. S1). ^{1}H NMR spectra (Figure S2) confirmed the complete removal of TOAB in $Au_{25}(PET)_{18}$.

To evaluate the stabilization capability of S-G, we used undoped graphene nanoplatelets (G) as a reference substrate for comparison. After purification of Au_{25}, the loading process was conducted by stir-mixing NCs and supporting materials in toluene at RT for 1 hour. Transmission electron microscopy (TEM) shows the overall size and uniformity of as-loaded Au_{25}. As shown in figure 1d, Au_{25} NCs were uniformly distributed on S-G with an ultrafine average size of 1.35 ± 0.45 nm based on statistical analysis (inset of Fig. 1d). In contrast, NCs loaded on graphene substrates show a significant trend toward aggregation. Nanoparticles with sizes ranging from 2~4 nm could be readily identified on the TEM image (Figure 1e). This aggregating phenomenon on graphene can be attributed to the lack of interacting species. $Au_{25}(PET)_{18}$ can interact with the substrate only via π- π conjugation between the phenylethanethiol (PET) staple ligand and graphene.

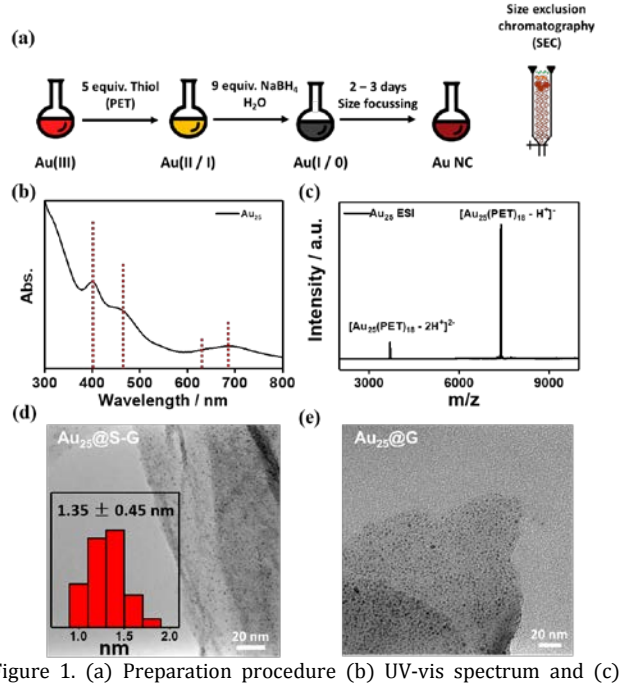

Figure 1. (a) Preparation procedure (b) UV-vis spectrum and (c) ESI-MS of as-synthesized $Au_{25}(PET)_{18}$ clusters. Typical TEM images of $Au_{25}(PET)_{18}$ clusters loaded on (d) sulfur-doped graphene and (e) graphene. The inset histogram of Fig, 1d shows the size distribution.

3.2 The electrocatalytic NRR tests of Au_{25}@ S-G and Au_{25}@G

We performed the nitrogen reduction reaction in 0.05 M H_2SO_4 electrolyte to evaluate the electrocatalytic property and stability of the Au_{25}@S-G composites. Au mass loading was determined to be to 11 μg/cm^2 for both Au_{25}@S-G and Au_{25}@G (confirmed by inductively coupled plasma mass spectrometry). A graphite rod and an Ag/AgCl (WPI, 3M KCl) electrode were used as a counter electrode and reference electrode, respectively. The ammonia yield rate was determined by UV–Vis absorption spectra of the electrolyte stained with commercial indophenol indicator (TNT830) after 3h NRR operations under various electrochemical potentials. The concentration of NH^{4+} in the electrolyte was calibrated by a commercial standard ammonia solution. The standard plot shows a highly linear relationship between absorbance and concentration (Figure S3 a-c). As shown in figure 2a, Au_{25}@S-G exhibits a peak NH_3 yield rate of 27.5 μg NH_3 $mg_{Au}^{-1}h^{-1}$ at -0.5 V with a faradic efficiency (FE) of 2.3%. This Au mass-normalized production rate is among the highest for previously reported Au-based NRR electrocatalysts [19] [20] [21]. When the operation potential was made more negative, both the ammonia production rate and the FE dropped dramatically due to the competing hydrogen evolution reaction (HER). As background reference, the NRR catalytic test with S-G alone shows negligible ammonia yield under the same electrochemical testing condition (Figure S4a and b). HAADF-STEM (Figure 2b and 2c) was used to monitor the morphology change between pristine Au_{25} and post-NRR Au_{25}. In this side-by-side comparison, the size and distribution of NCs on S-G remain mostly unchanged after 3 hours of NRR operation. The blurred substrate in the STEM image (Figure 2c) was induced by the addition of Nafion when preparing the electrode.

To detect trace amounts of ammonia, quantitative isotope measurement is needed to rule out potential contamination from the surrounding environment [22]. We conducted $^{15}N_2$ isotope labeling experiments to confirm that the source of nitrogen species in NH_4^+ generated comes from the N_2 feed gas (Figure S5a-c). We note that a set of tiny $^{14}NH_4^+$

background triplet peaks appear in the NMR spectra (Figure S5c). These peaks could be attributed to the 2-3% $^{14}N_2$ impurity in the $^{15}N_2$ isotope gas tank from the vendor.

Stability tests of Au_{25}@S-G and Au_{25}@G were conducted by chronoamperometry (CA) with operation potentials at -0.3 V vs. RHE. The tests were paused every 24h to analyze ammonia concentration in the catholyte, and the electrolyte was refreshed before resuming operation. The initial NRR activity of Au_{25}@S-G was 9.5 μg NH_3 $mg_{Au}^{-1}h^{-1}$ at -0.3 V with a faradic efficiency (FE) of 4.9%, while Au_{25}@G exhibited 2.28 μg NH_3 $mg_{Au}^{-1}h^{-1}$ catalytic activity at -0.3 V with a faradic efficiency (FE) of 1.85%. The ammonia production rate (R) was normalized by the initial rate ($R_{initial}$) at different times to compare the trend in stability. As shown in Figure 2d, The NH_3 yield rate for Au_{25}@S-G drops ~4% per day for the first 96 hours. In contrast, a dropping rate of ~20% activity was observed for the Au_{25}@G sample. TEM characterizations of post-test samples showed that S-G supported NCs (Figure 2e) maintained impressive dispersity and morphology even after 96 h catalytic operation. Whereas Au_{25}@G (Figure 2f) leads to NCs suffering from severe agglomeration in the post durability test.

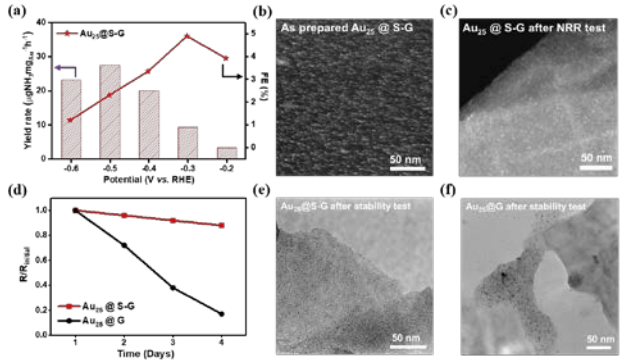

Figure 2. (a) Production rate of Au_{25}@S-G, faradaic efficiency of Au_{25}@S-G at different potentials for 3 h tests. The star was referring to the FE, and the histogram represents the ammonia yield rate. HAADF-STEM image of the (b) as-prepared Au_{25}@S-G and (c) Au_{25}@S-G post electrolysis in 0.05 M H_2SO_4 at -0.3V for 3h. (d) Stability test of Au_{25}@S-G and Au_{25}@G, respectively. TEM images of (E) Au_{25}@S-G and (F) Au_{25}@G post 96 hours NRR stability test.

3.3 The origin of the enhanced stability of Au_{25}@S-G configuration

Ex-situ X-ray photoelectron spectroscopy (XPS) was used to probe the chemical state of Au species after interacting with the sulfur-doped substrate. The XPS result for pristine Au_{25} NCs (Figure 3a) shows that the chemical state of Au in pristine clusters is predominately Au^0, which is consistent with previous spectroscopy studies [23] [24]. After loading the NCs on S-G, the XPS of the Au_{25}@S-G composite shows increasing Au^{x+} peaks with a binding energy of 86 eV and 89.6 eV for the Au 4f core-level region (labeled as a blue dot in Figure 3b), which we attribute to the interaction between sulfur-dopant on S-G with Au_{25} NCs. After conducting NRR at -0.3V for 3 h, the XPS for the post-reaction Au_{25}@S-G shows a slightly increased Au^{x+} ratio (Figure 3c) compared with as-loaded NCs. This result indicates that the chemical state of the Au NCs is stable during catalytic operation, reflecting a strong interaction between sulfur dopant and NCs.

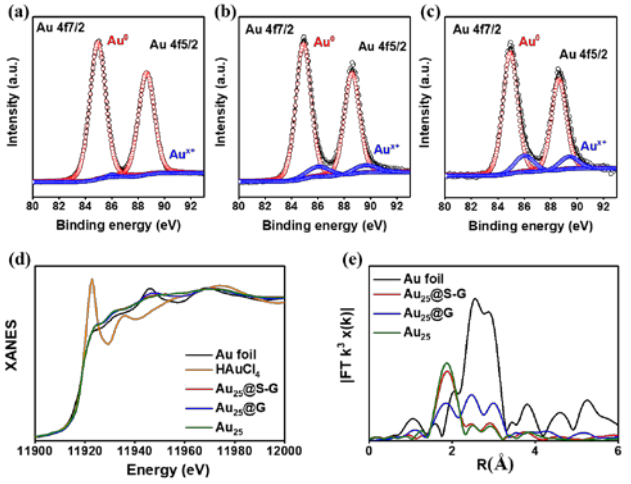

Figure 3. X-ray photoelectron spectroscopy of (a) as-synthesized $Au_{25}(PET)_{18}$ clusters, (b) as-loaded Au_{25}@S-G and (c) Au_{25}@S-G post NRR test. (d) XAS and (e) Au L_3 edge FT-EXAFS of Au_{25}@S-G and Au_{25}@G post 3-hour NRR test at -0.3V *vs.* RHE, with Au foil and $Au_{25}(PET)_{18}$ as the reference.

To investigate the interaction mechanism and to probe local Au atomistic and electronic structure, we conducted extended X-ray absorption fine structure (EXAFS) and X-ray absorption near-edge structure (XANES) measurements on Au_{25}@S-G and Au_{25}@G post 3h NRR tests at -0.3 V *vs.* RHE. The white line intensity probes the oxidation state of Au at the Au L-edge in XANES spectra. The Au XANES result shows that the white line intensities of both samples

(Figure 3d) are close to that of an Au foil, indicating that the average oxidation state of the NCs is close to a metallic state. The Au EXAFS (Figure 3e) fitting results shows an Au–Au bond length of 2.83 Å with CN = 1.1 (Table S1) for Au_{25}@S-G samples, which is in line with the value for pure Au_{25} and for the predicted Au_{13} icosahedral core group (Au–Au bond length 2.78, CN 1.44) in a previous structural study [25]. Moreover, both Au_{25}@S-G and Au_{25} show a Au-S bond length of 2.32 Å with similar Au-S CN (1.8 of Au_{25}@S-G and 1.9 of Au_{25}). Combined with our XPS result, we conclude that the sulfur dopant on S-G partially replaces the thiol ligand to bind with outer Au atoms. This result also demonstrates that the Au_{25}@S-G can maintain the coordination characteristics of $Au_{25}(PET)_{18}$ even after the catalytic process.

In contrast, the EXAFS result for Au_{25}@G shows an Au–Au bond length 2.86 with CN of 4.1 post NRR, indicating that aggregation has caused Au_{25} to lose cluster characteristics, getting closer to the bulk system. Additionally, comparing Au_{25}@S-G with pristine Au_{25}, the decreased Au-S coordination number (1.5 of Au_{25}@G *vs.* 1.8 of Au_{25}@S-G and 1.9 of Au_{25}) is plausible due to the ligand loss during sintering. This result shows that the monodispersed nanocluster without anchoring species on graphene aggregate during a dynamic electrocatalytic process.

To further reveal the sulfur-dopant role in stabilizing Au NCs, we carried out atomistic simulations using the reactive force field (ReaxFF). Based on the experimental results, we constructed two optimized models for computation study: 1) $Au_{25}(PET)_{18}$ on graphene (Figure 4a); 2) $Au_{25}(PET)_{18}$ on sulfur-doped graphene, with one ligand on the cluster replaced by a sulfur-dopant (Figure 4b). We calculated the binding energies of the two structures (Table S2), finding a binding energy of 2.23 eV for Au_{25}@G, and a binding energy of 7.11eV for Au_{25}@S-G. Therefore, the interaction of Au NCs with S-G is 4.88 eV stronger, consistent with experimental observations. More importantly, this stronger interaction will help prevent cluster aggregation. To prove this point, we carried out molecular dynamics simulations for Au_{25} dimers on these surfaces, at 298K for 2 ns. The simulation results (Movie S1-2) show that in 2 ns of ReaxFF molecular dynamics (RMD) simulation, sintering occurs for Au_{25}@G, but not for Au_{25}@S-G model(Figure S6). This shows that the enhanced binding can indeed play a role in stabilizing the Au NCs. These two observations are of the most importance in promoting catalysis performance and stability.

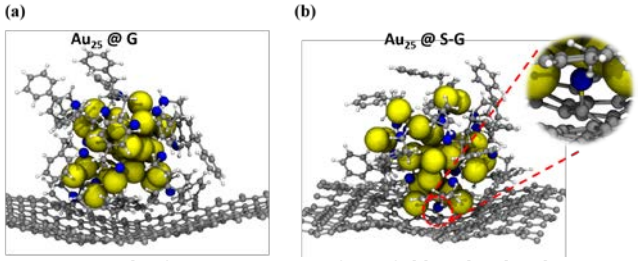

Figure 4. Results from 2ns reactive force field molecular dynamics (RMD) simulations followed by geometry optimization. Snapshots of (a) $Au_{25}(PET)_{18}$ on graphene and (b) $Au_{25}(PET)_{18}$ on sulfur-doped graphene, with one ligand on cluster replaced by sulfur-dopant after anchoring.

4 Conclusion

In conclusion, we successfully demonstrated that sulfur-doped graphene can stabilize ultrafine Au clusters for long term NRR electrocatalysis. The Au_{25}@S-G catalysts exhibit a high ammonia production rate of 27.5 $\mu g NH_3\ mg_{Au}^{-1} h^{-1}$ with a faradic efficiency of 2.3 % at - 0.5 V. More importantly, the NCs maintain an 80% NRR yield rate after the 96 h stability test without morphology destruction. *Ex-situ* TEM and STEM characterizations highlighted the remarkable structural stability of the Au_{25}@S-G composite. XPS and EXAFS studies support the stabilized chemical state and coordination status of NCs after interacting with S-G. It would be interesting to extend this work, to consider substrates with other chemical dopants (e.g., N, P) to be utilized as an anchoring platform to probe the ultrafine NC intrinsic electrocatalytic behavior. This study may contribute to bridge the gap between conventional nanoparticles [20] [21]and molecular single atomic catalysts[19], to provide electrocatalytic mechanism insight about ultrafine nanoclusters.

Acknowledgements

This research was supported by Director, Office of Science, Office of Basic Energy Sciences, Chemical Sciences, Geosciences, & Biosciences Division, of the US Department of Energy under Contract

DEAC02-05CH11231, FWP CH030201 (Catalysis Research Program). The Advanced Light Source is supported by the Director, Office of Science, Office of Basic Energy Sciences, of the US Department of Energy under Contract DE-AC02-05CH11231. This work made use of the facilities at the NMR Facility, College of Chemistry, University of California, Berkeley. Inductively coupled plasma optical emission spectrometry was supported by the Microanalytical Facility, College of Chemistry, University of California, Berkeley. Part of this material (WAG, TC) is based on work performed by the Liquid Sunlight Alliance, which is supported by the U.S. Department of Energy, Office of Science, Office of Basic Energy Sciences, Fuels from Sunlight Hub under Award Number DE-SC0021266.

This work is dedicated to the occasion of 80th birthday for Prof. Yitai Qian. As the undergraduate advisor for one of the authors (PY), Prof. Qian has had profound impact on this author's career in the field of materials chemistry. PY would like to acknowledge the unconditional support, encouragement and guidance from Prof. Qian back in early 1990s. It was during that time PY started his journey in solid state chemistry, by working on high temperature cuprate superconductors and finishing his undergraduate thesis on this exciting topic. The title page of this thesis was attached here (dated June 10, 1993).

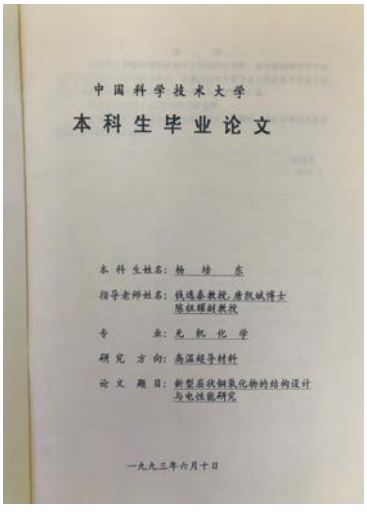
中国科学技术大学

本科生毕业论文

本科生姓名: 杨 培 东

指导老师姓名: 钱逸泰教授、唐凯斌博士
陈红耀副教授

专 业: 无 机 化 学

研究方向: 高温超导材料

论文题目: 新型层状铜氧化物的结构设计
与电性能研究

一九九三年六月十日

Electronic Supplementary Material: Supplementary material (further details of the EXAFS fitting, computational method, ^{1}H NMR for purified $Au_{25}PET_{18}$ clusters, UV-Vis calibration curves for ammonia determination, isotope labeling NMR result, optimized coordinates for simulation model) is available in the online version of this article at http://dx.doi.org/10.1007/10.1007/s12274-***-****-* (automatically inserted by the publisher) and is accessible free of charge

References

[1] Liu, L.; Corma, A. Metal catalysts for heterogeneous catalysis: From single atoms to nanoclusters and nanoparticles. *Chem Rev* **2018,** *118*, 4981-5079.

[2] Liu, L.; Corma, A. Confining isolated atoms and clusters in crystalline porous materials for catalysis. *Nature Reviews Materials* **2020**.

[3] Taylor, K. J.; Pettiette - Hall, C. L.; Cheshnovsky, O.; Smalley, R. E. Ultraviolet photoelectron spectra of coinage metal clusters. *The Journal of Chemical Physics* **1992,** *96*, 3319-3329.

[4] <jp026731y.Pdf>.

[5] Buceta, D.; Piñeiro, Y.; Vázquez-Vázquez, C.; Rivas, J.; López-Quintela, M. Metallic clusters: Theoretical background, properties and synthesis in microemulsions. *Catalysts* **2014,** *4*, 356-374.

[6] Zhu, Y.; Qian, H.; Drake, B. A.; Jin, R. Atomically precise au25(sr)18 nanoparticles as catalysts for the selective hydrogenation of alpha,beta-unsaturated ketones and aldehydes. *Angew Chem Int Ed Engl* **2010,** *49*, 1295-8.

[7] Zhang, H.; Liu, H.; Tian, Z.; Lu, D.; Yu, Y.; Cestellos-Blanco, S.; Sakimoto, K. K.; Yang, P. Bacteria photosensitized by intracellular gold nanoclusters for solar fuel production. *Nat Nanotechnol* **2018,** *13*, 900-905.

[8] Austin, N.; Zhao, S.; McKone, J. R.; Jin, R.; Mpourmpakis, G. Elucidating the active sites for co2 electroreduction on ligand-protected au25 nanoclusters. *Catalysis Science & Technology* **2018,** *8*, 3795-3805.

[9] Kauffman, D. R.; Thakkar, J.; Siva, R.; Matranga, C.; Ohodnicki, P. R.; Zeng, C.; Jin, R. Efficient electrochemical co2 conversion powered by renewable energy. *ACS Appl Mater Interfaces* **2015,** *7*, 15626-32.

[10]Kim, H. Y.; Lee, H. M.; Henkelman, G. Co oxidation mechanism on ceo(2)-supported au

nanoparticles. *J Am Chem Soc* **2012,** *134*, 1560-70.

[11]Zhang, B.; Chen, C.; Chuang, W.; Chen, S.; Yang, P. Size transformation of the au22(sg)18 nanocluster and its surface-sensitive kinetics. *J Am Chem Soc* **2020,** *142*, 11514-11520.

[12]Vilhelmsen, L. B.; Walton, K. S.; Sholl, D. S. Structure and mobility of metal clusters in mofs: Au, pd, and aupd clusters in mof-74. *J Am Chem Soc* **2012,** *134*, 12807-16.

[13]Dou, L.; Wu, S.; Chen, D.-L.; He, S.; Wang, F.-F.; Zhu, W. Structures and electronic properties of au clusters encapsulated zif-8 and zif-90. *The Journal of Physical Chemistry C* **2018,** *122*, 8901-8909.

[14]Li, J.; Wang, W.; Chen, W.; Gong, Q.; Luo, J.; Lin, R.; Xin, H.; Zhang, H.; Wang, D.; Peng, Q. et al. Sub-nm ruthenium cluster as an efficient and robust catalyst for decomposition and synthesis of ammonia: Break the “size shackles”. *Nano Research* **2018,** *11*, 4774-4785.

[15]Liu, L.; Diaz, U.; Arenal, R.; Agostini, G.; Concepcion, P.; Corma, A. Generation of subnanometric platinum with high stability during transformation of a 2d zeolite into 3d. *Nat Mater* **2017,** *16*, 132-138.

[16]Hakkinen, H. The gold-sulfur interface at the nanoscale. *Nat Chem* **2012,** *4*, 443-55.

[17]Burgi, T. Properties of the gold-sulphur interface: From self-assembled monolayers to clusters. *Nanoscale* **2015,** *7*, 15553-67.

[18]Kauffman, D. R.; Alfonso, D.; Matranga, C.; Qian, H.; Jin, R. Experimental and computational investigation of au25 clusters and co2: A unique interaction and enhanced electrocatalytic activity. *J Am Chem Soc* **2012,** *134*, 10237-43.

[19]Qiu, Y.; Peng, X.; Lu, F.; Mi, Y.; Zhuo, L.; Ren, J.; Liu, X.; Luo, J. Single-atom catalysts for the electrocatalytic reduction of nitrogen to ammonia under ambient conditions. *Chem Asian J* **2019,** *14*, 2770-2779.

[20]Wang, H.; Yu, H.; Wang, Z.; Li, Y.; Xu, Y.; Li, X.; Xue, H.; Wang, L. Electrochemical fabrication of porous au film on ni foam for nitrogen reduction to ammonia. *Small* **2019,** *15*, e1804769.

[21]Liu, D.; Zhang, G.; Ji, Q.; Zhang, Y.; Li, J. Synergistic electrocatalytic nitrogen reduction enabled by confinement of nanosized au particles onto a two-dimensional ti3c2 substrate. *ACS Appl Mater Interfaces* **2019,** *11*, 25758-25765.

[22]Andersen, S. Z.; Colic, V.; Yang, S.; Schwalbe, J. A.; Nielander, A. C.; McEnaney, J. M.; Enemark-Rasmussen, K.; Baker, J. G.; Singh, A. R.; Rohr, B. A. et al. A rigorous electrochemical ammonia synthesis protocol with quantitative isotope measurements. *Nature* **2019,** *570*, 504-508.

[23]Zhang, P. X-ray spectroscopy of gold–thiolate nanoclusters. *The Journal of Physical Chemistry C* **2014,** *118*, 25291-25299.

[24]Mathew, A.; Varghese, E.; Choudhury, S.; Pal, S. K.; Pradeep, T. Efficient red luminescence from organic-soluble au(2)(5) clusters by ligand structure modification. *Nanoscale* **2015,** *7*, 14305-15.

[25]MacDonald, M. A.; Chevrier, D. M.; Zhang, P.; Qian, H.; Jin, R. The structure and bonding of au25(sr)18 nanoclusters from exafs: The interplay of metallic and molecular behavior. *The Journal of Physical Chemistry C* **2011,** *115*, 15282-15287.

Electronic Supplementary Material

Sulfur-doped Graphene Anchoring of Ultrafine Au25 Nanoclusters for Electrocatalysis

Mufan Li [1,3,#], Bei Zhang[1,#], Tao Cheng[5], Sunmoon Yu[2,3], Sheena Louisia[1,3], Chubai Chen[1], Shouping Chen[2], Stefano Cestellos-Blanco[2], Miquel Salmeron[3], William A. Goddard III[5], Peidong Yang[1,2,3,4*](✉)

[1] Department of Chemistry, University of Berkeley, California 94720, United States
[2] Department of Materials Science and Engineering, University of Berkeley, California 94720, United States
[3] Chemical Science Division, Lawrence Berkeley National Laboratory, Berkeley, California 94720, United States
[4] Kavli Energy NanoScience Institute, Berkeley, California 94720, United States
[5] Materials and Process Simulation Center, California Institute of Technology, Pasadena, California 91125, United States

Supporting information to DOI 10.1007/s12274-****-****-* (automatically inserted by the publisher)

EXAFS fitting details

S_0^2 is the amplitude reduction factor; CN is the coordination number; R is the interatomic distance (the bond length between central atoms and surrounding coordination atoms); σ^2 is Debye-Waller factor (a measure of thermal and static disorder in absorber-scatterer distances); ΔE_0 is an edge-energy shift (the difference between the zero kinetic energy value of the sample and that of the theoretical model). R factor is used to value the goodness of the fitting.

* This value was fixed during EXAFS fitting, based on the known structure.

Error bounds that characterize the structural parameters obtained by EXAFS spectroscopy were estimated as N ± 20%; R ± 1%; σ^2 ± 20%; ΔE_0 ± 20%.

Au_{25}@S-G (FT range: 2.0-11.0 $Å^{-1}$; fitting range: 1.0-3.2 Å)

Au_{25}@G (FT range: 2.0-11.0 $Å^{-1}$; fitting range: 1.2-3.4 Å)

Au_{25} (FT range: 2.0-11.0 $Å^{-1}$; fitting range: 1.0-3.2 Å)

Au foil (FT range: 2.0-11.0 $Å^{-1}$; fitting range: 1.6-3.4 Å)

Table S1. Structural parameters extracted from the Au L_3-edge EXAFS fitting. (S_0^2=0.82)

sample	Scattering pair	CN	R(Å)	$\sigma^2(10^{-3}Å^2)$	ΔE_0(eV)	R factor
Au_{25}@S-G	Au-S	1.8	2.32	8.7	2.5	0.003
	Au-Au	1.1	2.83	11.3	2.5	
Au_{25}@G	Au-S	1.5	2.31	8.2	2.5	0.005
	Au-Au	4.1	2.86	10.1	2.5	
Au_{25}	Au-S	1.9	2.32	9.1	2.5	0.004

	Au-Au	0.9	2.84	12.2	2.5	
Au foil	Au-Au	12*	2.86	7.8	4.3	0.004

Computational simulation

We used the Large-scale Atomic/Molecular Massively Parallel Simulator (LAMMPS), version 7 Aug 2019 (DOI:10.1006/jcph.1995.1039) with the implementation of USER-REAXC package and fix qeq/reax (DOI:10.1016/j.parco.2011.08.005). The force field parameters to describe Au, C, S, and H is from the work of Jarvi et al. (DOI:10.1021/jp201496x). Energy minimization was performed first using CG with the Polak-Ribiere version of the conjugate gradient (CG) algorithm. The minimization was considered converged when all the length of the global force vector is less than 1e-8 kcal/mol A. The Molecular Dynamics (MD) Simulations were performed with time integration on Nose-Hoover style non-Hamiltonian equations of, which are designed to generate positions and velocities sampled described by canonical (NVT) ensembles. The MD simulation time step was 0.25 fs. The thermostat used a damping time of 25 fs.

Movie S1, 2: ReaxFF molecular dynamics (RMD) simulation for the Au_{25}@S-G and Au_{25}@G systems.

Table S2. The calculated binding energy of Au25 loaded on graphene and Sulfur-doped graphene, respectively

	Sub-Au-PET	**Au-PET**	**Sub**	**$E_{binding}$ (eV)**
Graphene	**-4199.93**	**-1821.21**	**-2376.49**	**-2.23**
S-Graphene	**-4161.70**	**-1714.59**	**-2440.00**	**-7.11**

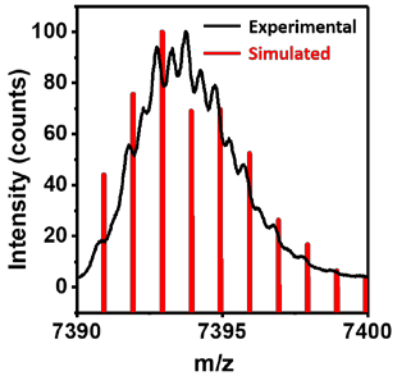

Figure S1. Simulated (red line) and experimental isotopic distribution ESI-MS patterns of $Au_{25}(PET)_{18}$.

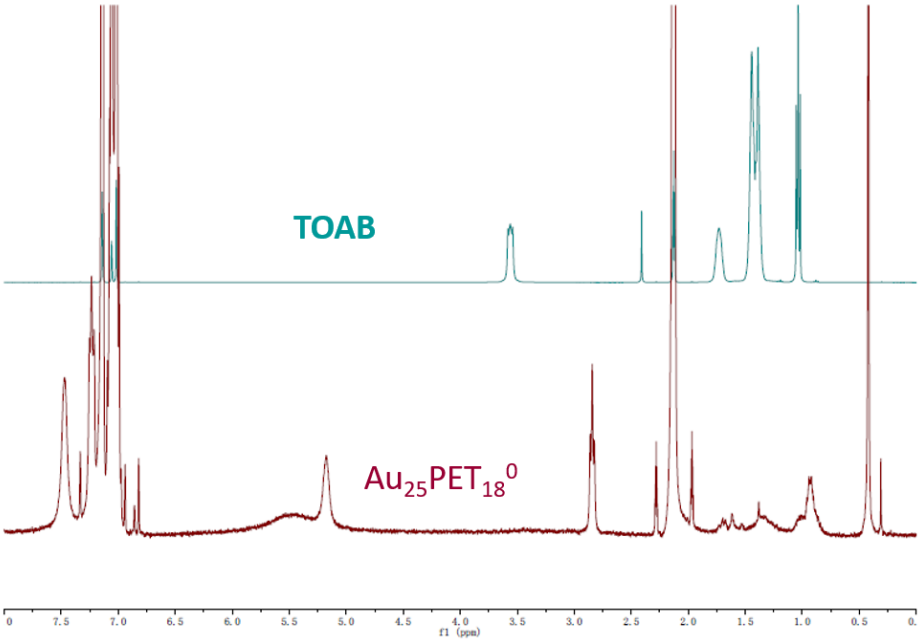

Figure S2. ^{1}H NMR spectra of TOAB and $Au_{25}PET_{18}$ neutral clusters.

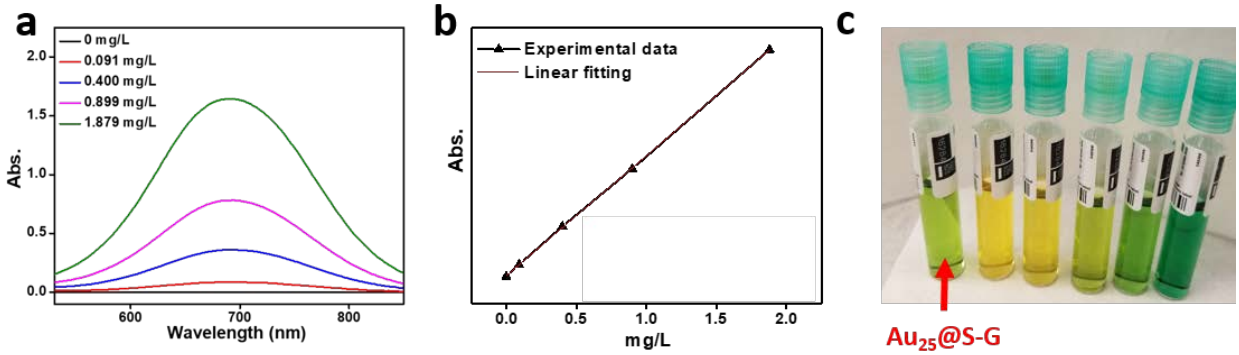

Figure S3. (a)UV-Vis spectrums for calibration ammonia solution with different concentrations. (b) The fitted curve used to calculate ammonia concentration. (c) Experimental sample and calibration standard using commercialized ammonia TNT830 vial test kit as the indicator.

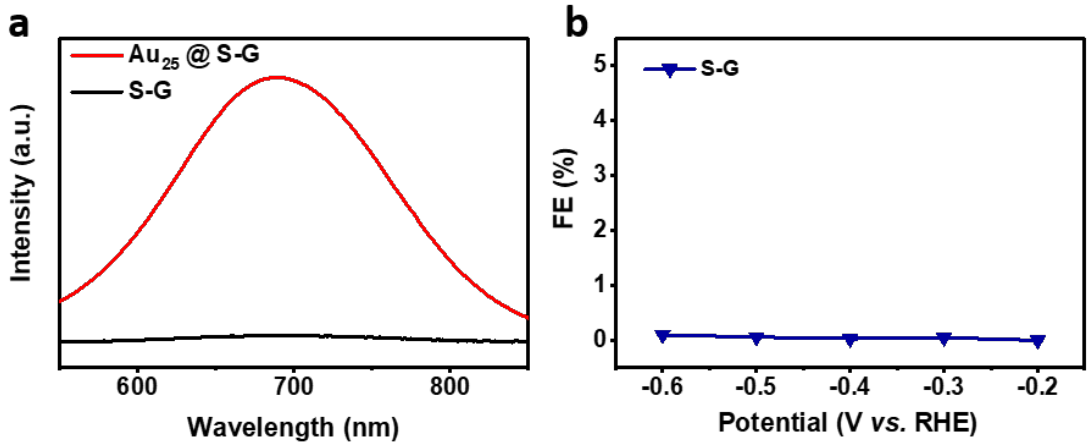

Figure S4. (a)UV-Vis spectrums of Au_{25}@S-G and S-G tested under -0.5V vs. RHE for 3h. (b) Faradaic efficiency towards ammonia on S-G at different potentials.

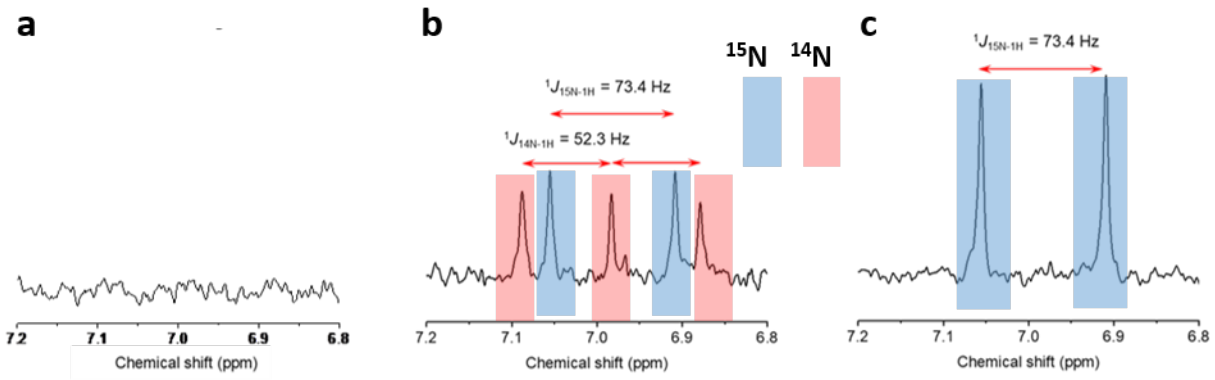

Figure S5. ^{1}H NMR spectra for (a) pure electrolyte, (b) 5 μM $^{15}NH_4^+$ + 5 μM $^{15}NH_4^+$ standard solution, and (c) post NRR (-0.5V vs. RHE for 3h) electrolyte with Au_{25}@S-G as the catalyst and $^{15}N_2$ as the feeding gas

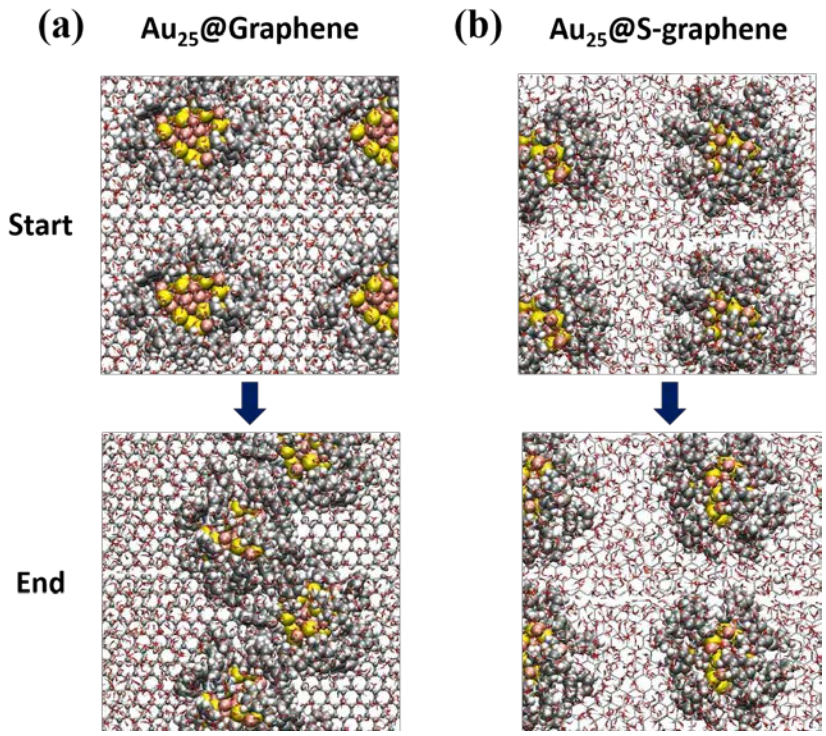

Figure S6. The snapshots of starting and ending stage of (a) Au_{25}@G and (b) Au_{25}@S-G in the simulation movie

Optimized coordinates for Au_{25}@G

637
40000

C	0.2645	0.1933	5.0504
C	1.4914	2.3508	4.7084
C	0.2719	1.6374	4.9894
C	1.3633	3.7294	4.2934
C	2.7363	0.1781	4.6486
C	3.8527	2.3253	4.0494
C	2.6891	1.6072	4.4973
C	3.7772	3.6660	3.5353
C	5.2124	0.1803	4.2897
C	6.2652	2.2268	3.3757
C	5.0889	1.5612	3.9111
C	6.1623	3.5629	2.8039
C	7.5907	0.1030	3.6582
C	8.6653	2.2618	2.8803
C	7.5243	1.5517	3.3684
C	8.6697	3.6448	2.4710
C	10.0316	0.1204	2.9396
C	11.1690	2.2390	2.6050
C	9.9439	1.5524	2.8034
C	11.1250	3.6992	2.5570
C	12.4861	0.1176	2.4656
C	13.6897	2.2719	2.4516
C	12.4398	1.5615	2.4176
C	13.6537	3.6747	2.5551

C	14.9914	0.1944	2.5632
C	16.1881	2.3387	3.0407
C	14.9656	1.5984	2.7370
C	16.1352	3.7565	3.0830
C	17.3736	0.1408	3.2964
C	18.6032	2.2911	3.6778
C	17.3625	1.6167	3.3539
C	18.5301	3.7143	3.7275
C	19.8239	0.1320	3.8809
C	21.0255	2.2945	4.2410
C	19.8244	1.5425	3.9747
C	20.9699	3.7400	4.3331
C	22.3062	0.1344	4.3723
C	23.4585	2.3237	4.8395
C	22.2457	1.5821	4.4893
C	23.4179	3.7603	4.8564
C	24.7505	0.1431	4.7511
C	25.9643	2.2762	5.0121
C	24.6852	1.5910	4.9279
C	25.8562	3.7253	4.9894
C	27.2650	0.1306	5.0628
C	28.4803	2.2571	4.8472
C	27.2165	1.5835	5.0461
C	28.3920	3.7003	4.7404
C	0.1236	4.4101	4.5106
C	1.3612	6.4881	3.7679
C	0.1357	5.7952	4.1481
C	1.4003	7.9487	3.7719
C	2.5305	4.3418	3.6439
C	3.7671	6.4651	3.1298
C	2.5495	5.7860	3.4749
C	3.8598	7.9202	3.2373
C	4.9381	4.3044	2.9679
C	6.1782	6.4558	2.4879
C	4.9970	5.7469	2.8858
C	6.2203	7.9279	2.4370
C	7.3578	4.2836	2.4298
C	8.5909	6.4371	1.9029
C	7.3589	5.6960	2.1911
C	8.6458	7.8759	1.8382
C	9.8872	4.4197	2.4438
C	11.1070	6.4912	2.1850
C	9.8521	5.8307	2.1543
C	11.1274	7.9471	2.0699
C	12.3931	4.3827	2.3573
C	13.5896	6.5897	2.6157
C	12.3654	5.8272	2.4399
C	13.6547	8.0124	2.3804
C	14.8667	4.4462	2.8360
C	16.0913	6.5806	2.9951
C	14.8322	5.8532	2.8263
C	16.1386	7.9692	2.6366

C	17.3846	4.4783	3.3323
C	18.5799	6.6066	3.4966
C	17.3336	5.9127	3.2764
C	18.5983	8.0217	3.1462
C	19.7415	4.4585	4.0425
C	21.0125	6.5776	4.0342
C	19.7578	5.8949	3.9393
C	21.0231	8.0242	3.7729
C	22.2075	4.4896	4.6114
C	23.4558	6.6571	4.4631
C	22.1912	5.8823	4.4118
C	23.4693	8.0986	4.3240
C	24.6686	4.4965	4.9559
C	25.9378	6.6192	4.7812
C	24.6636	5.9367	4.7361
C	26.0057	8.0439	4.5727
C	27.1353	4.4064	4.7579
C	28.4217	6.4832	4.4532
C	27.1158	5.8184	4.6636
C	28.5363	7.9020	4.5140
C	0.2323	8.6596	4.2643
C	1.5003	10.7643	4.1597
C	0.2351	10.0802	4.2950
C	1.4988	12.1897	4.1682
C	2.6518	8.6159	3.5980
C	3.8853	10.7870	3.3626
C	2.6926	10.0594	3.7430
C	3.9242	12.2200	3.4500
C	5.0341	8.6361	2.8149
C	6.2669	10.7904	2.5400
C	5.0558	10.0871	2.9043
C	6.3338	12.2137	2.6936
C	7.4078	8.6183	2.0349
C	8.7125	10.7812	1.9871
C	7.4567	10.0666	2.1600
C	8.7458	12.2007	2.1222
C	9.8826	8.6078	1.8632
C	11.2104	10.7006	1.6256
C	9.9127	10.0475	1.7282
C	11.2386	12.1683	1.6427
C	12.3927	8.6324	2.0077
C	13.7583	10.7566	1.6802
C	12.4880	10.0520	1.7443
C	13.7729	12.1855	1.7247
C	14.9410	8.6662	2.2180
C	16.2975	10.7512	1.9085
C	15.0044	10.0719	1.8958
C	16.2748	12.2159	1.9159
C	17.4118	8.6478	2.6758
C	18.6628	10.8357	2.5492
C	17.4676	10.0855	2.3309
C	18.7568	12.2742	2.3012

C	19.8259	8.7207	3.3490
C	21.0941	10.8611	3.2045
C	19.8305	10.1406	3.0691
C	21.1896	12.2415	2.8847
C	22.2411	8.7600	3.9162
C	23.5024	10.9057	3.8812
C	22.2803	10.1808	3.6077
C	23.5959	12.2893	3.5433
C	24.7456	8.7481	4.3704
C	26.0102	10.8135	4.3258
C	24.7354	10.1751	4.1649
C	26.0339	12.2490	4.1661
C	27.2964	8.6665	4.5535
C	28.4967	10.8276	4.4116
C	27.2697	10.0856	4.4174
C	28.5068	12.2718	4.3676
C	0.2745	12.9233	4.2960
C	1.5612	15.0417	4.4067
C	0.2983	14.3559	4.3389
C	1.5898	16.4687	4.5533
C	2.7243	12.9260	3.8355
C	3.9895	15.0862	3.7558
C	2.7671	14.3443	3.9600
C	4.0339	16.4461	4.1186
C	5.1551	12.9333	3.1728
C	6.3962	15.0629	3.0576
C	5.1854	14.3628	3.2555
C	6.4383	16.4659	3.4230
C	7.5648	12.9247	2.4865
C	8.8819	14.9981	2.7014
C	7.6049	14.3602	2.6545
C	8.9476	16.4065	3.0936
C	10.0733	12.8630	2.0024
C	11.3288	14.9829	2.1768
C	10.0700	14.2447	2.3481
C	11.3256	16.4262	2.3698
C	12.4944	12.8810	1.7072
C	13.8117	15.0334	1.7184
C	12.5473	14.3189	1.8547
C	13.8095	16.4750	1.8480
C	15.0184	12.9263	1.8036
C	16.3465	15.0712	1.7942
C	15.0638	14.3327	1.7375
C	16.3358	16.4923	1.8047
C	17.4972	12.9330	2.0875
C	18.8652	15.1248	1.8899
C	17.5734	14.3810	1.8924
C	18.8518	16.5528	1.8861
C	20.0156	12.9532	2.4625
C	21.2863	15.1172	2.3647
C	20.0437	14.3936	2.2121
C	21.3220	16.5416	2.3556

C	22.4471	12.9837	3.0789
C	23.6602	15.1108	3.2228
C	22.4471	14.4015	2.8771
C	23.7177	16.5396	3.0795
C	24.8623	12.9782	3.7731
C	26.0874	15.1184	3.9018
C	24.8624	14.4209	3.6675
C	26.0994	16.5662	3.7870
C	27.2593	13.0160	4.2796
C	28.5766	15.1232	4.4191
C	27.3093	14.4571	4.2494
C	28.5772	16.5602	4.4047
C	0.3362	17.1985	4.6477
C	1.6051	19.3366	4.8053
C	0.3482	18.6182	4.7537
C	1.6527	20.7873	4.9575
C	2.7981	17.2133	4.3399
C	4.1098	19.3155	4.5597
C	2.8411	18.6445	4.5389
C	4.1567	20.7647	4.7907
C	5.2704	17.1636	3.9455
C	6.6152	19.1939	4.3001
C	5.2908	18.5602	4.2965
C	6.6489	20.6336	4.5160
C	7.7487	17.0752	3.5194
C	8.9846	19.2556	3.6440
C	7.7805	18.5281	3.8289
C	9.0122	20.7115	3.7220
C	10.1826	17.1233	2.9134
C	11.3514	19.2698	2.8426
C	10.1479	18.5247	3.1597
C	11.3842	20.7226	2.9801
C	12.5525	17.1423	2.1312
C	13.7506	19.2965	2.1717
C	12.4974	18.5601	2.3162
C	13.7889	20.7184	2.3191
C	15.0503	17.1988	1.8786
C	16.2970	19.2992	1.8626
C	15.0018	18.6212	1.9901
C	16.2978	20.7594	2.0049
C	17.5681	17.2437	1.8240
C	18.8017	19.4466	2.1301
C	17.5687	18.6956	1.8505
C	18.7530	20.8189	2.4889
C	20.0655	17.2667	2.1613
C	21.2070	19.3507	2.8907
C	19.9835	18.6816	2.4189
C	21.2120	20.7724	2.9802
C	22.5085	17.2674	2.7171
C	23.6768	19.4217	3.3449
C	22.4677	18.6918	2.9635
C	23.6963	20.8443	3.4884

C	24.9307	17.2807	3.3687
C	26.1644	19.3819	3.8626
C	24.9321	18.7159	3.4864
C	26.1877	20.8073	4.1168
C	27.3470	17.2561	4.0757
C	28.6364	19.3807	4.4991
C	27.3896	18.6767	4.1753
C	28.6497	20.8005	4.5820
C	0.4064	21.4779	4.8184
C	1.5572	23.6119	5.0728
C	0.2993	22.9118	5.0209
C	1.5225	25.0217	4.9683
C	2.9045	21.4755	4.8811
C	4.0793	23.6101	4.8689
C	2.8199	22.9333	4.9406
C	4.0217	25.0585	4.6726
C	5.4385	21.3933	4.7878
C	6.4597	23.5328	4.2689
C	5.2979	22.8340	4.7735
C	6.4314	24.9727	4.1177
C	7.7846	21.3868	4.0963
C	8.7835	23.5543	3.3641
C	7.6338	22.7994	3.8764
C	8.8017	24.9873	3.3318
C	10.1846	21.4334	3.3290
C	11.2380	23.5433	2.6955
C	10.0342	22.8543	3.1605
C	11.2323	24.9841	2.6226
C	12.5391	21.4420	2.5789
C	13.7713	23.5731	2.3688
C	12.4987	22.8932	2.5657
C	13.7621	25.0046	2.3708
C	15.0423	21.4305	2.1710
C	16.2451	23.5724	2.6649
C	15.0275	22.8628	2.3398
C	16.2008	25.0163	2.8355
C	17.4926	21.4580	2.3734
C	18.6369	23.5904	3.2675
C	17.4811	22.8732	2.8217
C	18.5876	25.0090	3.5994
C	19.9626	21.5112	2.9486
C	21.1006	23.5902	3.7108
C	19.9215	22.9202	3.2670
C	21.1074	25.0040	4.0196
C	22.4136	21.4893	3.3643
C	23.5590	23.5499	4.1423
C	22.3885	22.9146	3.6204
C	23.5682	24.9974	4.3871
C	24.9162	21.4971	3.9227
C	26.0363	23.5720	4.6512
C	24.8308	22.8793	4.2814
C	26.0244	25.0287	4.7572

C	27.4010	21.5127	4.3818
C	28.5468	23.5790	5.0227
C	27.3204	22.9082	4.7748
C	28.5425	25.0403	5.0699
Au	11.8889	15.3006	11.5826
Au	9.4268	14.9812	13.2450
Au	10.2414	12.5344	15.0017
Au	12.8059	11.1187	13.3535
Au	9.3378	12.7172	9.1177
Au	11.6192	16.1684	8.2904
Au	13.3804	17.6575	10.4952
Au	14.6899	15.3077	12.5747
Au	10.6014	12.6816	12.0025
Au	8.0030	9.9434	8.5460
Au	10.2154	10.0006	6.4391
Au	14.3074	12.1053	8.8073
Au	15.0605	10.7085	11.2410
Au	16.8909	10.9825	8.5220
Au	16.3560	13.7949	7.6005
Au	14.2542	15.0893	9.5939
Au	15.3289	12.6399	13.5661
Au	15.1535	9.4318	14.0917
Au	13.7449	7.6305	11.8415
Au	12.2313	8.5288	8.0856
Au	16.2098	13.4717	10.7605
Au	17.4910	14.6900	13.1580
Au	15.0994	14.9266	15.5253
Au	12.6159	13.8314	13.9364
Au	13.3745	12.9574	11.3435
C	10.0507	18.0251	12.2462
C	8.5613	18.6638	12.8940
C	7.8533	17.7086	13.9523
C	8.4990	17.3594	15.1474
C	7.7129	16.6638	16.1540
C	6.2858	16.5132	15.9119
C	5.7906	16.6034	14.6191
C	6.5742	17.2098	13.6178
C	7.0716	13.3590	14.7700
C	6.5647	12.3165	16.0881
C	5.5873	13.2403	16.8674
C	6.0140	14.0604	17.9470
C	5.1013	14.8291	18.6908
C	3.7219	14.8105	18.3221
C	3.3162	14.0860	17.1790
C	4.2451	13.2854	16.4538
C	10.0849	9.0967	14.3272
C	8.7619	8.8546	15.3905
C	8.0804	7.5081	15.1493
C	6.8806	7.3130	14.3798
C	6.3728	6.0370	14.1551
C	7.1488	4.8875	14.5161
C	8.2811	5.0525	15.3266

C	8.6592	6.3598	15.7621
C	13.1770	18.9596	7.5338
C	12.1585	19.2231	6.0446
C	11.2296	20.4588	6.1864
C	9.8553	20.3956	6.5561
C	9.0568	21.5759	6.5036
C	9.6959	22.8055	6.1901
C	11.0889	22.8915	5.9598
C	11.8833	21.7015	5.9283
C	16.2678	18.1410	12.0048
C	16.1757	19.9555	11.7984
C	15.1488	20.5195	10.7468
C	13.7261	20.6597	10.9707
C	12.9298	21.1266	9.8562
C	13.5700	21.8307	8.7496
C	14.9465	21.7287	8.5579
C	15.7211	21.1146	9.6141
C	8.9669	14.9927	6.9447
C	8.4876	13.9036	5.6422
C	7.8556	12.6074	6.3174
C	7.9127	11.5154	5.4395
C	6.9194	10.3386	5.6048
C	5.7769	10.6212	6.6055
C	5.7820	11.7800	7.3797
C	6.8255	12.7750	7.3005
C	7.6408	11.1171	11.6720
C	7.0036	9.5117	12.2137
C	6.6494	8.6959	10.9475
C	5.5491	9.2053	10.2389
C	5.1346	8.5549	9.0220
C	5.9625	7.5587	8.4293
C	7.0709	7.0245	9.1906
C	7.4239	7.5456	10.4589
C	8.5227	7.2325	6.5361
C	9.4926	6.9096	5.1777
C	10.9832	6.8460	5.5390
C	11.9721	7.7601	4.9692
C	13.3345	7.5116	5.3640
C	13.7461	6.5125	6.2739
C	12.7338	5.6560	6.8595
C	11.3352	5.8534	6.4777
C	13.3993	10.9576	5.9164
C	12.5666	12.0658	4.7602
C	13.3193	13.3592	5.0184
C	12.4529	14.4714	5.2056
C	13.0554	15.7583	5.4586
C	14.4474	15.8591	5.2726
C	15.2795	14.7491	4.7824
C	14.7280	13.4618	4.8280
C	16.3821	8.0662	9.8980
C	17.6666	7.2690	8.9340
C	17.6696	8.0155	7.5662

C	16.4664	8.3360	6.8920
C	16.5194	9.2401	5.8255
C	17.8458	9.6735	5.4436
C	19.0876	9.0492	5.9431
C	18.9869	8.2387	7.0830
C	19.7502	11.9005	7.0812
C	19.9430	13.3535	7.9625
C	20.2101	14.4986	6.9210
C	21.3015	15.2749	7.3271
C	21.5636	16.5221	6.6807
C	20.8131	16.8490	5.5586
C	19.6831	16.0782	5.1164
C	19.3489	14.9180	5.8775
C	16.8682	16.9207	8.5869
C	18.0543	17.3030	7.3462
C	17.6151	18.6313	6.6937
C	16.7423	18.5317	5.5803
C	16.2907	19.7175	4.9534
C	16.6863	20.9642	5.4470
C	17.5885	21.0265	6.5256
C	18.1543	19.8629	7.1071
C	12.8819	7.2229	15.0745
C	13.3368	7.5996	16.8118
C	12.4037	8.6432	17.3058
C	11.5127	8.2866	18.3217
C	10.5361	9.2065	18.8286
C	10.5215	10.6013	18.5232
C	11.5098	11.1060	17.6717
C	12.3262	10.1406	16.7846
C	11.0750	6.5203	10.1195
C	10.9187	4.9019	10.7415
C	11.5083	4.7821	12.1979
C	12.8812	4.5926	12.3230
C	13.4978	4.3889	13.6549
C	12.6410	4.2288	14.7944
C	11.2419	4.3864	14.6038
C	10.6955	4.7615	13.3360
C	18.0308	10.8056	14.1581
C	18.6956	9.2760	14.7790
C	17.9541	8.1293	14.0125
C	18.2535	7.7293	12.6253
C	17.8209	6.4069	12.2380
C	17.0307	5.5903	12.9933
C	16.7070	6.0213	14.3258
C	17.2264	7.2921	14.8674
C	19.2081	12.3412	11.3652
C	20.9381	12.2885	11.9540
C	21.6580	11.8479	10.6630
C	22.4343	12.7082	9.8544
C	23.0720	12.2204	8.6926
C	22.9917	10.8518	8.3894
C	22.1638	10.0042	9.1758

C	21.4819	10.4844	10.3136
C	17.6095	16.9363	15.5909
C	19.3054	17.2613	15.3945
C	19.5605	17.1856	13.8223
C	19.2602	18.2709	12.9688
C	19.5474	18.1639	11.5653
C	20.1383	17.0034	11.0245
C	20.5660	15.9608	11.9243
C	20.2397	16.0707	13.3439
C	12.0524	16.0093	16.2309
C	12.4520	16.8355	17.7967
C	11.5533	16.2143	18.8967
C	12.1043	15.1957	19.7237
C	11.3057	14.4579	20.6295
C	9.9274	14.8160	20.6891
C	9.3550	15.8523	19.8850
C	10.1763	16.5490	18.9643
H	10.7954	17.7162	13.0334
H	10.5576	18.7128	11.4329
H	7.8519	18.7835	12.0804
H	8.7341	19.6648	13.3242
H	9.4696	17.7428	15.3683
H	8.1446	16.4908	17.1407
H	5.6269	16.1115	16.6588
H	4.7921	16.2585	14.4027
H	6.1341	17.2155	12.6047
H	6.3483	14.1511	14.4866
H	7.4749	12.8578	13.8656
H	6.1426	11.4493	15.7010
H	7.4405	11.9781	16.6751
H	7.0617	14.0282	18.2745
H	5.4705	15.4354	19.5054
H	3.0035	15.3991	18.8558
H	2.2879	14.0885	16.8637
H	3.9027	12.7272	15.5916
H	9.8886	9.7836	13.5037
H	10.6807	8.1875	14.0244
H	9.1389	8.7964	16.4008
H	8.0409	9.6846	15.3130
H	6.3146	8.1715	13.9936
H	5.4825	5.9187	13.5585
H	6.8977	3.9002	14.2007
H	8.8342	4.1571	15.5898
H	9.4995	6.4822	16.4126
H	13.6892	19.8761	7.9296
H	13.8000	18.0761	7.4810
H	11.4676	18.4181	5.7959
H	12.8317	19.3495	5.1746
H	9.4074	19.4160	6.6881
H	7.9980	21.5548	6.7377
H	9.0791	23.6803	6.1827
H	11.6222	23.8331	5.7609

H	12.9488	21.7166	5.6824
H	16.9976	17.8230	12.8141
H	16.4147	17.4907	11.1290
H	16.0068	20.3927	12.7466
H	17.1773	20.2196	11.4570
H	13.2734	20.4390	11.9256
H	11.8615	21.2835	9.9820
H	12.9500	22.3433	8.0301
H	15.3911	22.1790	7.6879
H	16.8077	21.0933	9.4947
H	8.2843	15.0496	7.8765
H	9.2309	15.9638	6.5539
H	7.6308	14.4376	5.0051
H	9.2442	13.6832	4.9149
H	8.4459	11.6591	4.5000
H	6.6646	9.8708	4.6248
H	5.0015	9.8951	6.7146
H	4.9114	12.0389	8.0460
H	6.7058	13.6647	7.9156
H	7.8339	11.7863	12.5718
H	6.9199	11.6481	11.0494
H	7.7527	9.0601	12.7973
H	6.1176	9.6564	12.8371
H	4.9388	10.0043	10.6725
H	4.1549	8.7766	8.6117
H	5.6860	7.0650	7.5103
H	7.5926	6.1993	8.7792
H	8.3048	7.2403	10.9750
H	9.1065	6.9523	7.4875
H	7.5480	6.6947	6.4554
H	9.1219	5.9408	4.7602
H	9.2810	7.6196	4.3583
H	11.7226	8.3395	4.1522
H	14.1531	7.9942	4.8693
H	14.7731	6.3655	6.5080
H	13.0720	4.8815	7.4854
H	10.6134	5.2170	6.8709
H	14.4322	11.3196	6.1144
H	13.4478	9.8981	5.5404
H	12.5162	11.7978	3.6929
H	11.5529	12.1452	5.1039
H	11.2976	14.3096	5.1275
H	12.4894	16.6022	5.5911
H	14.8947	16.8453	5.2115
H	16.2600	14.9237	4.4051
H	15.3534	12.5937	4.5446
H	15.4515	8.2513	9.3197
H	16.1615	7.4353	10.8882
H	18.7042	7.1849	9.3507
H	17.3571	6.2305	8.8279
H	15.4953	7.9962	7.2820
H	15.6486	9.6742	5.4985

H	17.9687	10.2521	4.5727
H	20.0725	9.2593	5.4940
H	19.9289	8.0260	7.5731
H	20.3424	11.8694	6.0903
H	19.8376	10.9461	7.6916
H	20.7466	13.1565	8.6717
H	19.0752	13.6094	8.6083
H	21.8318	15.1222	8.2156
H	22.3236	17.1959	7.0598
H	21.0391	17.8097	5.0718
H	19.0544	16.4534	4.3412
H	18.4440	14.3751	5.6583
H	17.2778	16.1790	9.3081
H	16.5086	17.8376	9.1199
H	18.0324	16.5565	6.5643
H	19.0819	17.3485	7.7263
H	16.5094	17.5783	5.1165
H	15.6469	19.7073	4.0773
H	16.3213	21.8823	5.0364
H	17.7647	21.9600	6.9484
H	18.8549	19.9391	7.9277
H	11.9987	6.5399	14.9347
H	12.6576	8.1689	14.5536
H	13.3103	6.6862	17.4037
H	14.3478	7.9012	16.7087
H	11.5120	7.2980	18.7216
H	9.8166	8.8999	19.5355
H	9.8177	11.2628	19.0708
H	11.5835	12.1127	17.4513
H	13.2441	10.5729	16.3861
H	10.3757	6.7413	9.2842
H	10.7054	7.2114	10.9111
H	11.4576	4.2193	10.0678
H	9.8342	4.6289	10.6875
H	13.5003	4.4825	11.4403
H	14.5995	4.2557	13.7479
H	13.0586	4.1445	15.7885
H	10.5853	4.2064	15.4555
H	9.6288	4.8675	13.1361
H	18.7308	11.6620	14.3554
H	17.6987	10.8045	13.0826
H	18.5059	9.1851	15.8352
H	19.7635	9.2572	14.6643
H	18.8424	8.2887	11.9645
H	18.1553	6.0425	11.2599
H	16.7077	4.6013	12.7085
H	16.1446	5.3684	14.9803
H	17.1961	7.4398	15.9352
H	19.0194	11.9272	10.3321
H	18.4774	11.8954	12.0858
H	20.9991	11.5728	12.7438
H	21.3164	13.2201	12.3787

H	22.5010	13.7406	10.1728
H	23.6702	12.8469	8.0695
H	23.5312	10.4618	7.5305
H	22.0957	8.9649	8.8560
H	20.8114	9.8412	10.8720
H	17.2205	17.2916	16.6121
H	16.9861	17.3849	14.7913
H	19.9230	16.4822	15.9135
H	19.5395	18.2783	15.8141
H	18.8240	19.1782	13.3887
H	19.3300	19.0264	10.9446
H	20.2773	16.9344	9.9607
H	21.1863	15.1335	11.5549
H	20.5364	15.3097	14.0409
H	10.9342	15.8135	16.1535
H	12.4434	16.5053	15.3091
H	12.2162	17.8853	17.6686
H	13.5173	16.7432	18.0230
H	13.1871	14.9972	19.7025
H	11.7471	13.6900	21.2414
H	9.2484	14.2989	21.3714
H	8.3103	16.0753	19.9185
H	9.7645	17.3612	18.3799
S	9.6427	16.6803	11.4090
S	8.3703	14.2531	15.4419
S	11.2909	10.0181	15.1887
S	12.0004	18.6998	8.6616
S	14.7779	17.9717	12.6450
S	10.4326	14.2094	7.3495
S	9.0674	10.7641	10.8375
S	7.9600	8.8491	6.4476
S	12.4189	11.0223	7.3595
S	17.0972	9.4463	10.5412
S	18.1024	11.9497	6.6559
S	15.6095	16.1064	7.7268
S	14.2220	6.8922	14.1341
S	12.6623	6.6852	9.6587
S	16.6619	11.0117	15.0671
S	18.8351	13.9484	11.2482
S	17.5600	15.2949	15.6755
S	12.7846	14.5224	16.4105

Au_{25}@S-G
619
178
C 21.8549 6.6305 3.2490
C 23.0333 8.8056 3.7188
C 21.8390 8.0711 3.3829
C 22.9810 10.2470 3.7119
C 24.3040 6.6937 3.5882
C 25.4494 8.8235 4.3560
C 24.2760 8.0991 3.9248
C 25.4178 10.2666 4.3547
C 26.7282 6.7022 4.2496
C 27.9259 8.8370 4.7680
C 26.6958 8.1155 4.5393
C 27.9030 10.2755 4.6602
C 29.2009 6.6835 4.6130
C 0.9109 8.8261 4.6594
C 29.1785 8.1179 4.7789
C 0.8975 10.2639 4.5735
C 2.1593 6.6912 4.3203
C 3.3834 8.8119 4.0647
C 2.1501 8.1310 4.3793
C 3.4038 10.2451 4.2066
C 4.6284 6.6766 3.7434
C 5.8537 8.8108 3.5358
C 4.5998 8.1177 3.6957
C 5.8692 10.2321 3.7883
C 7.1268 6.6528 3.6182
C 8.3554 8.7883 3.4790
C 7.0976 8.0841 3.4299
C 8.3440 10.2324 3.4517
C 9.5963 6.7174 4.0514
C 10.8419 8.8802 3.8933
C 9.6077 8.1344 3.7901
C 10.8534 10.2652 3.4814
C 12.0662 6.7861 4.4172
C 13.2937 8.9885 4.1484
C 12.0744 8.2280 4.2568
C 13.3177 10.3626 3.6680
C 14.5114 6.7611 4.3970
C 15.6706 8.8335 3.6599
C 14.5034 8.2066 4.2044
C 15.5997 10.0950 2.8181
C 16.9514 6.7096 4.1370
C 18.1023 8.7441 3.2247
C 16.9161 8.1178 3.7615
C 18.0907 10.0218 2.4085
C 19.3930 6.6258 3.6590
C 20.5843 8.7682 3.2062
C 19.3477 8.0503 3.3960
C 20.5501 10.1950 2.9664

C	21.7826	10.9044	3.2350
C	23.0209	13.0326	3.1706
C	21.7638	12.3326	3.0425
C	23.0041	14.4738	3.0524
C	24.2091	10.9583	3.9640
C	25.4807	13.0627	3.5928
C	24.2296	12.3523	3.5867
C	25.4842	14.4542	3.1972
C	26.6642	10.9838	4.4278
C	27.9378	13.0501	3.8418
C	26.6808	12.3658	4.0012
C	27.9502	14.4350	3.4359
C	29.1586	10.9729	4.5185
C	0.9136	13.0473	3.9385
C	29.1739	12.3577	4.1137
C	0.9339	14.4453	3.5858
C	2.1514	10.9535	4.3777
C	3.4268	13.0923	4.1318
C	2.1716	12.3803	4.1809
C	3.4284	14.5055	3.8399
C	4.6605	10.9505	4.1111
C	5.9339	13.1066	4.1215
C	4.6855	12.3886	4.2236
C	5.9115	14.5392	3.9386
C	7.1207	10.9519	3.7154
C	8.3674	13.0701	3.4750
C	7.1569	12.3865	3.8678
C	8.3589	14.5098	3.4144
C	9.5948	10.9369	3.2833
C	10.7759	13.0425	2.6027
C	9.5679	12.3697	3.0670
C	10.7774	14.5010	2.6915
C	12.0793	11.0110	3.2807
C	13.2848	13.0973	2.4886
C	12.0521	12.3343	2.6564
C	13.2435	14.5482	2.3867
C	14.5150	11.0594	3.2093
C	15.6675	13.3557	3.0560
C	14.5247	12.4441	2.7847
C	15.6826	14.6239	2.2605
C	16.8268	10.5116	2.4294
C	18.0174	13.0513	2.4386
C	18.0486	14.5406	2.6154
C	19.3241	10.8324	2.5790
C	20.5049	13.0133	2.8737
C	19.2836	12.2638	2.6075
C	20.4943	14.4277	3.1269
C	21.7429	15.1526	3.2361
C	23.0029	17.3062	3.4961
C	21.7694	16.5539	3.5831
C	22.9984	18.7137	3.8274
C	24.2522	15.1947	3.0344

C	25.4773	17.3571	3.1884
C	24.2269	16.6353	3.1335
C	25.4715	18.7716	3.4739
C	26.7297	15.1772	3.2075
C	27.9413	17.3143	3.5609
C	26.7185	16.6211	3.2300
C	27.9493	18.7113	3.9331
C	29.2035	15.1522	3.4271
C	0.9131	17.3150	3.6707
C	29.1916	16.5921	3.5300
C	0.9152	18.7121	4.0353
C	2.1773	15.1762	3.5690
C	3.3956	17.3665	3.3922
C	2.1656	16.6176	3.4766
C	3.3872	18.8019	3.5431
C	4.6655	15.2457	3.7638
C	5.8761	17.4010	3.2896
C	4.6491	16.6485	3.4184
C	5.8890	18.8466	3.3130
C	7.1315	15.2433	3.6322
C	8.3619	17.3879	3.3446
C	7.1130	16.6645	3.3726
C	8.3709	18.8172	3.5739
C	9.5746	15.2060	3.0670
C	10.8477	17.3123	3.5071
C	9.5935	16.6386	3.2757
C	10.8205	18.6773	3.9972
C	12.0216	15.2443	2.6749
C	13.2949	17.3377	3.2747
C	12.0572	16.6086	3.1603
C	13.2769	18.6433	3.9186
C	14.4401	15.3597	2.2832
C	15.7090	17.4922	2.8272
C	14.4775	16.7551	2.7078
C	15.7178	18.7682	3.5204
C	16.9006	15.3965	2.2089
C	18.1614	17.4346	3.1155
C	16.9671	16.8404	2.5174
C	18.1909	18.7643	3.7122
C	19.2592	15.1694	3.1684
C	20.5395	17.2424	3.8688
C	19.3078	16.5872	3.4565
C	20.5780	18.6324	4.2504
C	21.8149	19.3787	4.3149
C	23.0177	21.5577	4.4444
C	21.8119	20.7906	4.6318
C	23.0236	22.9837	4.6862
C	24.2225	19.4666	3.6852
C	25.4655	21.5850	3.9947
C	24.2057	20.8783	3.9807
C	25.4677	23.0135	4.1826
C	26.7070	19.4356	3.8177

C	27.9540	21.5387	4.3571
C	26.7157	20.8570	4.0570
C	27.9778	22.9780	4.2422
C	29.1815	19.3862	4.2702
C	0.9166	21.5356	4.5384
C	29.1905	20.8100	4.5096
C	0.9268	22.9725	4.3823
C	2.1678	19.4325	3.9886
C	3.4106	21.5599	4.2576
C	2.1612	20.8355	4.3275
C	3.4115	22.9945	4.4358
C	4.6334	19.5327	3.4905
C	5.8912	21.6161	4.1671
C	4.6535	20.9131	3.9125
C	5.8982	22.9786	4.6488
C	7.1281	19.5468	3.5497
C	8.3464	21.5626	4.4836
C	7.1410	20.9139	4.0212
C	8.3530	22.9500	4.8898
C	9.5915	19.4350	4.0291
C	10.8187	21.5039	4.7328
C	9.5786	20.8146	4.4625
C	10.8266	22.9526	4.7582
C	12.0629	19.3383	4.2837
C	13.2579	21.5107	4.5636
C	12.0397	20.7456	4.6358
C	13.2398	22.9367	4.2968
C	14.5103	19.3669	4.0256
C	15.6997	21.5330	4.4424
C	14.4824	20.7581	4.4338
C	15.6804	22.9691	4.2544
C	16.9442	19.4628	3.8471
C	18.1496	21.5363	4.7072
C	16.9476	20.8054	4.3926
C	18.1262	22.9845	4.7280
C	19.3534	19.3951	4.2865
C	20.5989	21.5202	4.9174
C	19.3789	20.7804	4.7202
C	20.5827	22.9630	5.0317
C	21.8085	23.7145	4.9551
C	23.0428	0.3223	4.6069
C	21.8163	25.1553	4.7956
C	23.0600	1.7020	4.1649
C	24.2486	23.7224	4.4925
C	25.5271	0.2906	4.2660
C	24.2898	25.1662	4.5532
C	25.5442	1.7154	4.0340
C	26.7367	23.7073	4.1382
C	28.0078	0.2531	3.7379
C	26.7654	25.1483	4.0519
C	28.0241	1.6908	3.5941
C	29.2250	23.6995	4.1487

C	0.9822	0.2411	3.6300
C	29.2534	25.0952	3.7661
C	0.9866	1.6818	3.5086
C	2.1660	23.7084	4.2760
C	3.4504	0.2575	4.1550
C	2.2051	25.1147	3.9500
C	3.4501	1.6926	4.0425
C	4.6534	23.7106	4.6131
C	5.8773	0.2841	4.9134
C	4.6496	25.1538	4.6095
C	5.8730	1.7236	4.8013
C	7.1170	23.6872	4.9596
C	8.3641	0.2814	5.0104
C	7.1153	25.1272	5.0805
C	8.3595	1.7211	4.8792
C	9.5985	23.6858	4.9185
C	10.7720	0.2475	4.3193
C	9.5980	25.1276	4.8072
C	10.7789	1.6891	4.2026
C	12.0091	23.6792	4.3561
C	13.1759	0.2246	3.6165
C	11.9856	25.0909	4.0269
C	13.1864	1.6722	3.5635
C	14.4450	23.6616	3.9765
C	15.6748	0.2055	3.5709
C	14.4221	25.0644	3.6107
C	15.6493	1.6483	3.4682
C	16.9233	23.6868	4.3250
C	18.1465	0.2148	4.0732
C	16.8918	25.0851	3.9527
C	18.1260	1.6201	3.7287
C	19.3549	23.7114	4.8769
C	20.5853	0.2842	4.5062
C	19.3439	25.1196	4.5458
C	20.6091	1.6343	3.9829
C	21.8365	2.3664	3.7898
C	23.0803	4.4944	3.2388
C	21.8536	3.7388	3.3289
C	23.1169	5.9408	3.2417
C	24.2892	2.4194	3.9283
C	25.5421	4.5685	3.5993
C	24.3135	3.8040	3.5103
C	25.5552	6.0058	3.7672
C	26.7810	2.4065	3.7420
C	28.0085	4.5804	3.9573
C	26.7836	3.8527	3.7227
C	27.9728	5.9783	4.3308
C	29.2681	2.4195	3.5345
C	0.9402	4.5598	4.0763
C	29.2389	3.8359	3.8289
C	0.9170	5.9639	4.4242
C	2.2218	2.3913	3.7323

C	3.4150	4.5466	4.0623
C	2.1754	3.8210	3.9307
C	3.3942	5.9915	4.0331
C	4.6585	2.3965	4.4025
C	5.9005	4.5669	4.1915
C	4.6596	3.8306	4.2364
C	5.8785	5.9477	3.7661
C	7.1177	2.4529	4.8383
C	8.3530	4.5909	4.3552
C	7.1183	3.8609	4.5104
C	8.3586	5.9817	3.9646
C	9.5830	2.4151	4.5543
C	10.8324	4.5899	4.3445
C	9.5948	3.8599	4.4636
C	10.8378	6.0391	4.3454
C	11.9867	2.4062	3.8740
C	13.2686	4.5858	4.1270
C	12.0370	3.8382	4.0910
C	13.2847	6.0157	4.3947
C	14.4258	2.4073	3.5442
C	15.6921	4.5513	4.0360
C	14.4631	3.8212	3.8700
C	15.7216	5.9844	4.2831
C	16.8900	2.3611	3.5964
C	18.1543	4.5050	3.8213
C	16.9002	3.7944	3.8203
C	18.1605	5.9457	3.9736
C	19.3793	2.3288	3.6833
C	20.6081	4.4643	3.3114
C	19.3634	3.7713	3.5384
C	20.6064	5.9084	3.3523
Au	11.9684	16.5822	10.5335
Au	9.2878	15.0173	9.7444
Au	11.4882	13.1711	5.5578
Au	12.6593	10.3189	9.3020
Au	17.7000	12.6056	7.8170
Au	17.4665	17.2335	8.7686
Au	14.5189	17.7545	9.3115
Au	13.3706	12.2235	11.6876
Au	14.2425	14.3745	5.8061
Au	16.9451	15.7360	5.3395
Au	17.2454	11.1793	5.0727
Au	18.2140	10.5963	9.9378
Au	15.7877	6.9387	11.2909
Au	18.3864	9.3927	14.7872
Au	19.5523	13.1607	9.9791
Au	16.8949	14.5375	9.9223
Au	13.8618	14.5051	9.7462
Au	10.3499	11.6963	11.3685
Au	12.7979	7.3652	10.7745
Au	14.3279	11.3626	6.5290
Au	17.0959	11.3879	12.9498

Au	16.5311	14.0521	15.9457
Au	12.2073	14.7681	14.8841
Au	11.2228	12.9340	9.0308
Au	15.3959	11.8799	9.5137
C	9.1751	17.8901	11.2040
C	7.6414	17.7281	10.3041
C	6.7186	17.3286	11.4677
C	6.5426	18.2986	12.4947
C	5.7917	17.9656	13.6418
C	5.1937	16.6817	13.7432
C	5.3711	15.7189	12.7149
C	6.1439	16.0299	11.5729
C	8.4088	13.3420	6.9345
C	6.9715	14.4050	7.1079
C	6.0050	13.3884	7.7612
C	4.7000	13.3634	7.2018
C	3.7128	12.5232	7.7658
C	4.0396	11.7016	8.8768
C	5.3501	11.7218	9.4237
C	6.3365	12.5806	8.8826
C	10.4876	10.2100	6.7734
C	9.6073	9.7166	8.1513
C	8.5941	8.7028	7.6456
C	8.9329	7.3182	7.6808
C	7.9712	6.3644	7.2888
C	6.6871	6.7891	6.8515
C	6.3685	8.1724	6.7857
C	7.3195	9.1382	7.1765
C	16.4261	20.4473	9.7410
C	16.9097	20.3097	8.0280
C	18.4670	20.1236	7.9773
C	19.2964	20.9964	8.7239
C	20.7007	20.8210	8.7001
C	21.2867	19.7615	7.9483
C	20.4767	18.9274	7.1505
C	19.0711	19.1633	7.0872
C	15.1721	16.1140	12.3471
C	15.9526	16.6761	13.8438
C	16.5355	18.0320	13.5523
C	17.8632	18.3182	13.9368
C	18.3666	19.6338	13.8226
C	17.5146	20.7131	13.4288
C	16.1804	20.4693	13.1034
C	15.7441	19.1011	12.9410
C	19.9107	14.2452	6.5164
C	21.0101	15.2658	6.8365
C	22.3855	14.5145	6.8411
C	23.5046	15.3473	7.0712
C	24.7980	14.7700	7.1196
C	24.9551	13.3708	6.9494
C	23.8233	12.5424	6.7284
C	22.5287	13.1144	6.6619

C	12.0569	16.9701	7.1249
C	12.1648	18.6909	7.1855
C	10.7110	19.1591	7.1837
C	9.6330	18.2582	6.9363
C	8.3100	18.7411	6.9845
C	8.0695	20.1197	7.2333
C	9.1499	21.0140	7.4609
C	10.4773	20.5363	7.4538
C	17.6603	8.8666	7.1958
C	19.2147	9.3000	6.7252
C	20.2220	8.1931	7.0815
C	21.5640	8.6066	7.3118
C	22.5664	7.6251	7.4731
C	22.2191	6.2481	7.4375
C	20.8676	5.8474	7.2610
C	19.8565	6.8185	7.0812
C	14.6002	9.2810	13.6903
C	14.6607	8.9426	15.4139
C	14.7608	7.3891	15.4634
C	16.0226	6.7875	15.1942
C	16.0752	5.4185	14.8322
C	14.8901	4.6412	14.9022
C	13.6521	5.2368	15.2625
C	13.5715	6.6269	15.5281
C	20.4966	10.0300	12.3335
C	21.3680	10.8637	10.9669
C	22.6890	10.1068	11.0037
C	22.7287	8.7629	10.5345
C	23.9291	8.0349	10.6673
C	25.0763	8.6557	11.2321
C	25.0332	10.0088	11.6652
C	23.8358	10.7455	11.5561
C	19.0846	16.0320	11.8977
C	20.1948	16.1876	10.5669
C	21.0428	17.3964	10.9628
C	20.4654	18.6561	11.2864
C	21.3259	19.6908	11.7103
C	22.7274	19.4650	11.7892
C	23.2867	18.2024	11.4536
C	22.4424	17.1542	11.0366
C	11.3412	9.1022	13.3363
C	10.6743	7.5186	13.3248
C	9.2011	7.7097	13.0135
C	8.7267	7.8929	11.6806
C	7.3356	7.9619	11.4573
C	6.4308	7.8548	12.5496
C	6.9147	7.7098	13.8775
C	8.3021	7.6510	14.1180
C	14.5479	7.9459	8.0418
C	12.9058	7.3256	7.5752
C	13.1729	5.8667	7.8693
C	12.4003	5.0888	8.8161

C	12.8528	3.7883	9.1649
C	13.9719	3.2317	8.5076
C	14.6680	3.9610	7.5000
C	14.2774	5.2749	7.1894
C	9.1859	13.5071	14.0016
C	8.9046	12.2851	15.3193
C	7.4139	12.3324	14.8874
C	6.5621	13.2167	15.5922
C	5.1822	13.2392	15.2807
C	4.6778	12.4009	14.2521
C	5.5519	11.5517	13.5233
C	6.9312	11.5112	13.8405
C	19.2072	13.2978	14.3998
C	19.7056	14.5013	15.6773
C	21.1789	14.2586	15.4552
C	21.9171	15.1200	14.5889
C	23.2574	14.8042	14.2959
C	23.8556	13.6426	14.8571
C	23.1088	12.7819	15.7075
C	21.7687	13.0847	16.0139
C	14.1733	12.2795	14.8316
C	13.5380	13.0301	17.6870
C	13.1191	11.4866	17.7858
C	14.0953	10.5278	18.1466
C	13.7038	9.1714	18.2892
C	12.3581	8.7925	18.0478
C	11.4021	9.7566	17.6361
C	11.7837	11.1162	17.4995
C	11.9565	17.8309	13.7628
C	10.8245	18.2762	15.0712
C	11.6239	17.8173	16.3305
C	11.2268	16.6972	17.1280
C	11.9092	16.4393	18.3558
C	12.9452	17.2989	18.7845
C	13.3218	18.4199	17.9929
C	12.6706	18.6678	16.7596
H	9.0409	18.4559	12.1512
H	9.9728	18.3639	10.6000
H	7.6732	17.0108	9.4887
H	7.3747	18.6834	9.8521
H	7.0050	19.2688	12.4044
H	5.6750	18.6897	14.4355
H	4.6024	16.4377	14.6123
H	4.9162	14.7430	12.8090
H	6.2938	15.2945	10.7983
H	8.5455	12.9695	5.8921
H	8.4692	12.4991	7.6631
H	7.1613	15.2621	7.7535
H	6.6239	14.7965	6.1538
H	4.4593	13.9946	6.3608
H	2.7142	12.5117	7.3536
H	3.2852	11.0626	9.3090

H	5.5914	11.0862	10.2631
H	7.3207	12.6153	9.3214
H	9.8849	10.7724	6.0418
H	11.0306	9.3936	6.2698
H	10.2582	9.2674	8.8922
H	9.1245	10.5723	8.6156
H	9.9046	7.0041	8.0215
H	8.2099	5.3106	7.3238
H	5.9535	6.0551	6.5582
H	5.3942	8.4847	6.4364
H	7.0817	10.1881	7.1385
H	15.3994	20.8229	9.8934
H	17.1712	20.9803	10.3665
H	16.6205	21.2409	7.5350
H	16.3679	19.5179	7.5093
H	18.8601	21.7878	9.3128
H	21.3330	21.4835	9.2696
H	22.3552	19.6078	7.9729
H	20.9208	18.1435	6.5604
H	18.4501	18.5684	6.4237
H	15.7457	16.4586	11.4522
H	14.1045	16.3936	12.2770
H	15.2096	16.7070	14.6402
H	16.7343	16.0101	14.1717
H	18.4922	17.5421	14.3484
H	19.3933	19.8421	14.0801
H	17.8924	21.7257	13.4202
H	15.5358	21.2755	12.8105
H	14.6988	18.8995	12.6918
H	20.0308	13.2679	6.9773
H	19.6014	14.1526	5.4810
H	21.0017	16.0804	6.1118
H	20.8433	15.7259	7.8132
H	23.3666	16.4081	7.2138
H	25.6585	15.3970	7.2939
H	25.9409	12.9337	6.9886
H	23.9525	11.4772	6.6006
H	21.6729	12.4822	6.4811
H	12.0361	16.5324	6.1106
H	11.2673	16.5408	7.7692
H	12.6669	19.0652	8.0689
H	12.7452	19.0756	6.3525
H	9.8191	17.2239	6.7084
H	7.4846	18.0647	6.8132
H	7.0595	20.4936	7.2303
H	8.9600	22.0650	7.6198
H	11.3074	21.2039	7.6187
H	17.5988	8.3196	8.1492
H	17.0731	8.3456	6.4227
H	19.2530	9.4925	5.6551
H	19.5193	10.2334	7.1986
H	21.8154	9.6547	7.3305

H	23.5940	7.9239	7.6224
H	22.9885	5.5016	7.5525
H	20.6126	4.7977	7.2563
H	18.8317	6.5232	6.9262
H	13.9808	8.5390	13.1339
H	14.3018	10.3106	13.4082
H	15.4928	9.4457	15.9242
H	13.7332	9.2939	15.9017
H	16.9157	7.3797	15.1509
H	17.0120	4.9777	14.5228
H	14.9374	3.5873	14.6806
H	12.7613	4.6322	15.3135
H	12.6254	7.1068	15.7283
H	20.8536	8.9235	12.4161
H	20.5621	10.5613	13.3126
H	21.5025	11.9241	11.1613
H	20.8644	10.7296	10.0136
H	21.8494	8.3059	10.1097
H	23.9731	7.0046	10.3441
H	25.9899	8.0936	11.3342
H	25.9136	10.4724	12.0868
H	23.7830	11.7676	11.8939
H	19.6099	16.1585	12.8645
H	18.2096	16.7123	11.8493
H	19.6915	16.3151	9.6198
H	20.8405	15.3218	10.4664
H	19.3999	18.8085	11.2313
H	20.9171	20.6548	11.9762
H	23.3780	20.2601	12.1121
H	24.3518	18.0370	11.5204
H	22.8408	16.1839	10.7862
H	10.5982	9.8875	13.5405
H	12.2375	9.2275	13.9613
H	11.1475	6.8591	12.6128
H	10.8212	7.0582	14.2967
H	9.4152	7.9561	10.8546
H	6.9542	8.0842	10.4527
H	5.3681	7.8829	12.3710
H	6.2224	7.6352	14.7042
H	8.6824	7.5323	15.1187
H	15.3448	7.1791	8.1128
H	14.8751	8.7897	7.4193
H	12.7156	7.5262	6.5221
H	12.0797	7.7565	8.1359
H	11.5147	5.5101	9.2834
H	12.3341	3.2255	9.9252
H	14.3016	2.2374	8.7645
H	15.5059	3.5174	6.9823
H	14.8236	5.8494	6.4573
H	8.5428	13.3853	13.0795
H	9.2112	14.5809	14.3186
H	9.1230	12.6702	16.3167

H	9.3890	11.3170	15.1694
H	6.9598	13.8492	16.3700
H	4.5157	13.8875	15.8296
H	3.6230	12.4095	14.0250
H	5.1619	10.9265	12.7350
H	7.6002	10.8593	13.3010
H	19.9495	13.2767	13.5750
H	19.1238	12.2684	14.8107
H	19.3489	14.2208	16.6632
H	19.3848	15.5139	15.4573
H	21.4507	15.9869	14.1540
H	23.8298	15.4445	13.6397
H	24.8831	13.4089	14.6322
H	23.5669	11.8918	16.1155
H	21.1843	12.4281	16.6365
H	15.0565	11.6602	15.0124
H	13.2220	11.7452	14.7677
H	12.7117	13.7435	17.8317
H	14.4166	13.3135	18.2873
H	15.1189	10.8261	18.3184
H	14.4312	8.4270	18.5743
H	12.0613	7.7619	18.1719
H	10.3841	9.4584	17.4365
H	11.0654	11.8602	17.1928
H	11.9515	18.5725	12.9359
H	13.0035	17.6732	14.0966
H	9.8471	17.7909	14.9869
H	10.6539	19.3570	15.0643
H	10.3894	16.0778	16.8281
H	11.6210	15.6002	18.9683
H	13.4463	17.1149	19.7243
H	14.0962	19.0879	18.3377
H	12.9428	19.5297	16.1688
S	9.7703	16.4017	11.7415
S	9.7574	14.3236	7.2865
S	11.8570	11.3092	7.1505
S	16.4566	18.9019	10.3825
S	15.1300	14.4255	11.9419
S	17.8750	15.0543	7.5528
S	13.4326	16.0439	7.7962
S	16.3353	13.3946	4.6516
S	16.7213	10.4231	7.5679
S	16.1683	8.9686	13.1147
S	18.8604	9.6780	12.1977
S	18.4720	14.4651	11.9976
S	12.0051	9.6415	11.7698
S	14.6321	8.6024	9.6550
S	10.7052	13.0990	13.5360
S	17.6969	13.6687	13.7766
S	14.0750	13.4533	15.9689
S	11.3030	16.4027	13.1953